



Notre Dame University - Louaize
Faculty of Natural & Applied Sciences
Department of Sciences
MS Biology Program

Customized D2B coated Gold Nanoparticles: Promising Targeting Agents against Prostate Cancer

Prepared by
Monira Sarkis

Supervised by
Dr. Esther Ghanem

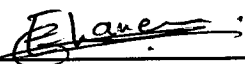
*A thesis submitted to Notre Dame University
Faculty of Natural & Applied Sciences in partial fulfillment
of the Master Degree requirements in Biology*

Spring 2018

Customized D2B coated Gold Nanoparticles: Promising Targeting Agents against Prostate Cancer

Certificate of Examination

Thesis Advisor: Dr. Esther Ghanem



Committee Member: Dr. Kamil Rahme



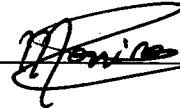
Committee Member: Dr. Diala El-Khoury



Thesis Release Form

I Monica Saksis, authorize Notre Dame University-Louaize to supply copies of my thesis to libraries or individuals on request.

I _____, do not authorize Notre Dame University-Louaize to supply copies of my thesis to libraries or individuals on request.



Signature

May 21, 2018.

Date

“Trust in dreams, for in them is hidden the gate to eternity ...”

Gebran Khalil Gebran

Acknowledgements

With boundless love and appreciation, I would like to extend my heartfelt gratitude to each and every person that helped me throughout the bouncy road of my master's thesis.

Primarily, I would like to extend my profound acknowledgment to the following:

My sweet advisor **Dr. Esther Ghanem**, whom without, none of this would have been possible and whose expertise, ample time, constant guidance and infinite support allowed the study to come to reality and mold it into the masterpiece that it is. Your door was always open whenever I ran into trouble and you never failed to help me put all the missing pieces of my work together and keeping the flow harmonious even after your call of duty.

A special gratitude to **Dr. Kamil Rahme**, for always managing to steer the work in the right direction and for making it a beautiful journey to embark on. Thank you for the fruitful discussions, critical comments, and the constant encouragement you showered us with. A special thank you to **Dr. Diala El Khoury** for playing a decisive role in providing the insightful suggestions and corrections of the thesis and that added to the benefit of the study.

My genuine and warmest appreciation also goes to all the lab members, and most importantly **Mrs. Nada Maalouf** and **Mrs. Elizabeth Saliba**, for their countless assistance and providing a helping hand whenever needed. Your beautiful spirits harbored a joyful environment to work with. I also owe a special thanks to my research partner **Mr. Georges Minassian** who has been like a brother to me. Thank you for contributing invaluable to this work and for your beautiful companionship; you have always managed to put a smile on my face.

A warm thank you also goes to Professors **Hassan Naim** and **Giulio Fracasso** for their generous support and continuous feedback all throughout the work progress. I would also like to thank the **CNRS** for their partial coverage of the thesis work and ofcourse the **FNAS** for the complete support and providing the platform to conduct all my research.

I am greatly indebted to everyone who has contributed to this work and most importantly to the *Notre Dame University* for being my second home.

And finally, words prove a meagre media to write down my sincerest feelings for my family who have tolerated my stressful days and uplifted me during my lowest moments. If it weren't for you I wouldn't have reached that far.

THANK YOU

Monira Sarkis

Abstract

Gold nanoparticles (AuNPs) with an estimate diameter of 25 nm have been synthesized and characterized using ultraviolet-visible spectroscopy (UV-Vis), dynamic light scattering (DLS) and Zeta potential measurements. AuNPs were coated with D2B, a monoclonal antibody recognizing an extracellular epitope of the human prostate specific membrane antigen (hPSMA). Binding of D2B to PSMA induces endocytosis of the latter, thereby marking PSMA as a docking site for the delivery of therapeutic agents. To attain a stabilized and covalent bond between D2B and AuNPs, the sulfhydryl group (SH) in a cysteine of the D2B was utilized. Binding of D2B to AuNPs-citrate colloidal solution caused a red shift with a higher wavelength of about 15 nm in the UV-Vis spectra. Furthermore, as a confirmation of the successful conjugation, DLS revealed an increase in both the AuNPs size from 25 to ~63 nm and Zeta potential measurements for AuNPs-citrate from -45 mV to -23 mV. The cytotoxicity of D2B-AuNPs was assessed using the WST-1 cell proliferation assay and the agarose gel DNA fragmentation method. Finally, specific delivery and binding of D2B-AuNPs was tested using flow cytometry and western blot. Our results pave the way for further research using coated NPs as vehicles for drug delivery in both *in vitro* and *in vivo* models.

Table of Contents

List of Tables	ix
List of Figures	x
List of abbreviations.....	xi
I. Introduction	1
II. Literature Review	8
1. Background on Prostate Cancer	9
1.1 Causes and Risk Factors of Prostate Cancer.....	10
1.2 Screening and Diagnosis of prostate cancer	10
1.3 Current Treatments	11
2. Targeted Therapy and Nanotechnology	12
2.1 Theranostic NP applications for Prostate Cancer	16
2.1.1 Iron Oxide Nanoparticles	16
2.1.2 Gadolinium, Manganese, Silver, and Platinum	17
2.1.3 Quantum Dots.....	19
2.1.4 Liposomes	20
2.2 Gold Nanoparticles (AuNPs).....	22
III. Materials and Methods.....	28
1. Chemicals	28
2. Synthesis of Gold Citrate (AuNP-Citrate) Nanoparticles.....	29

3. UV-Visible Spectroscopy analysis.....	29
4. Dynamic Light Scattering and Zeta Potential measurements.....	29
5. Cell Culture.....	30
7. DNA Fragmentation	31
8. Flow Cytometry.....	31
9. Western Blot	32
10. Statistical Analysis.....	33
IV. Results.....	34
1. Synthesis and Characterization of AuNPs-D2B.	35
2. WST-1 Cell Proliferation Assay.....	35
3. DNA Fragmentation	35
4. Flow Cytometry Analysis.....	36
5. Western Blot	37
V. Discussion	38
VI. Conclusion.....	50
VIII. Tables and.....	61
Figures.....	61

List of Tables

Table 1. Summary of the gold nanoparticles employed for the targeted therapy or diagnosis of prostate cancer.....	66
---	----

List of Figures

Figure 1: UV-Visible spectra of AuNPs-Citrate (~25 nm) before and after bioconjugation with D2B	69
Figure 2: Size distribution by number from DLS on (~25 nm) AuNPs-Citrate before and after bioconjugation with D2B.....	69
Figure 3: Effect of gold nanoparticles (AuNP) on PC3-PSMA proliferation.....	3
Figure 4: Effect of gold nanoparticles conjugated to D2B antibody (AuNP-D2B) on PC3-PSMA proliferation.....	4
Figure 5: DNA analysis of the PC3-PSMA cells treated with increasing concentrations of AuNP-D2B.....	72
Figure 6: Typical representative histogram of AuNP-D2B binding to PC3-PSMA.....	72
Figure 7: FACS analysis of AuNP-D2B binding to PC3-PSMA	73
Figure 8: Western Blot Analysis for PSMA expression and AuNP-D2B binding.....	74
Figure 9: A stepwise schematic representation of a targeted photothermal therapy on PSMA expressing prostate cancer cells.....	75
Figure 10: A schematic figure illustrating the surface plasmon resonance.....	76
Figure 11: A representative image of the antibody binding onto the gold nanoparticles..	76
Figure 12: A schematic figure representation of the internalization of PSMA targeted AuNP-D2Bs.....	77
Figure 13: Figure sketch representing the PSMA Structure.....	77

List of abbreviations

µg	Microgram
PCa	Prostate Cancer
PSMA	Prostate-specific membrane antigen
RPMI	Roswell Park Memorial Institute
SDS-PAGE	sodiumdodecylsulfate-polyacrylamide gel electrophoresis
SDS	sodiumdodecylsulfate
AuNP	Gold Nanoparticles
AuNP-D2B	Gold Nanoparticles conjugated to D2B
mAb	monoclonal antibody
DLS	Dynamic Light Scattering
RIT	Radioimmunotherapy
DRE	Digital rectal exam
CT	Computer tomography
PSA	Prostate specific antigen
MRI	Magnetic Resonance Imaging
SPION	Superparamagnetic Iron Oxide Nanoparticles
PEG	Polyethylene glycol
AgNP	Silver Nanoparticles
QD	Quantum Dots
DOX	Doxorubicin
HRP	Horserraddish peroxidase

PTT	Photothermal therapy
PC3-WT	Wild type human prostate cancer
PC3-PSMA	human prostate cancer over-expressing PSMA
EGC	Epigallocatechin gallate
HSP 90	Heat shock protein 90

I. Introduction

Prostate cancer (PCa) has become a common tumor affecting men, with a high risk above the age of 50 years. In the U.S. alone, prostate cancer is the second leading cause of death in men. Its incidence is largely correlated to age, [1] and therefore it is more commonly found in elder men at advanced stages [2]. With millions of people suffering from this disease annually, [3] treatment and management of prostate has become a definitive obligation for researchers. Traditional approaches for prostate cancer treatment encompass cancer radical prostatectomy, external beam radiation therapy (EBRT), and brachytherapy mainly through the insertion of radioactive implants directly into the tumor tissue; however, such approaches and other allied treatments, although manifest short term remission, but also result in recurrence of the cancer due to acquiring resistive capabilities and this remains a challenging issue and a common argument in the arena of efficient tumor treatment and eradication methodologies. To date, there is no treatment that has been proven to be ideal, patients are often advised to weigh the risks before committing to their choice of treatment [4]. Usually cancers are characterized by their inherent genomic instability, heterogeneity, and rapid tumor evolution which eventually will lead to the proliferation of the cancer and results in its aggressiveness. Therefore, treatments must act before the cancer cells can take their toll on the human health and adapt by acquiring resistance.

Nevertheless, despite the magnitude of therapy options available to treat cancers, effective and safe tumor progression management measures, continue to be unmet. It is therefore, necessary to devise a more targeted approach and many methods have been sought in order to treat prostate cancer [5, 6]. Currently chemotherapy is applied systemically for patients who have prostate cancer that has undergone metastasis, [7] and this tends to affect healthy tissues along with the tumor of interest; hence, resulting in

undesirable side effects of treatment [8, 9]. Consequently, there remains a pressing need to further explore the use of targeted therapy in prostate cancer. The new approach for treatment should tackle a more targeted strategy in which the drug or biochemical therapeutic is designed to specifically localize and induce selective killing in tumors. This is referred to as the “magic bullet” approach in which it basically involves the binding of a specific protein receptor that is over-expressed in a tumor, to a drug that is conjugated to a targeting ligand [8]. Prostate cancer diagnosis has been greatly aided since the discovery of the prostate specific antigen (PSA). PSA is an androgen-regulated serine protease produced by both prostate epithelial cells and prostate cancer (PCa). It is a major protein in semen, where its function is to cleave semenogelins in the seminal coagulum [10].

PSA that enters the circulation intact is rapidly bound by protease inhibitors. This proteolytic inactivation, is less efficient in PCa [11]. Unfortunately, although high PSA levels is a governing factor of advanced PCa, a large fraction of cancers are paralleled with much lower total PSA values [12].

These culminating reasons, therefore drive scientists to seek alternative markers for the prognosis and treatment of prostate cancer since PSA has recently indicated that it may have additional roles in the pathogenesis of PCa by enhancing its progression [11].

In addition, some scientists have come to a unified realization that it is rather PSMA that beholds the prognostic and therapeutic significance. In a study implemented by Murphy *et. al.*, 1996 the authors have come to a conclusion that PSMA and not PSA was largely correlated to the stages of prostate cancer. As, stated in their study, they believe that PSA can be derived from non-malignant cells such as prostatitis [13].

Interestingly, the putative over expression of PSMA in prostate cancer serves as an attractive and ideal candidate for effective targeting and treatment. Many papers have reported the use of anti-PSMA antibodies as therapeutic treatments for prostate cancer and combination with gene therapy was also a trending subject for researchers [14].

Among the various proteins associated with prostate cancer such as laminin receptor [15], notch receptor, [16] and Androgen receptor, [17] prostate-specific membrane antigen (PSMA) was shown through screening techniques to be mostly implicated in the diagnosis, management and treatment of the disease [3, 18]. PSMA is a characteristic cell-surface marker of prostate cancer and is found to be over-expressed in the advanced stages of the tumor [19]. The role of PSMA as an enzyme serves as a great advantage for PCa cells growth, since PSMA hydrolyzes the extracellular polyglutamated folate to mono-glutamic folic acid that is then used by the cells [2]. Moreover, recently, the group of J. Grimm has demonstrated that PSMA activates oncogenic signaling stimulating the metabotropic glutamate receptors by means of the cleavage of vitamin B9. [20]

This cell-surface protein comprised of 750 amino acids is a significant indicator for disease outcome [21] and it is known as glutamate carboxypeptidase II, N-acetyl-L-aspartyl-L-glutamate peptidase I, and folate hydrolase.

What truly marks PSMA as an exquisite candidate for prostate treatment, apart from its proven overexpression and restriction to prostate cells, is conceivably the internalization motif that it has and which plays a pivotal role in better tumor penetration and internalization of therapeutic agents [22, 23].

For this particular reason, we sought to design PSMA targeted gold nanoparticles (AuNPs) that could later on be used for the treatment of PCa when conjugated to an

effective therapeutic payload. Over the years multiple nanosystems have been evaluated for the treatment of cancer; however, our interest in AuNPs mainly emerged due to their significant translational potential in cancer therapy, biocompatibility, small size, and most importantly their safety [24]. Many studies have reported the use of AuNPs for prostate cancer treatment and imaging [25] and have taken advantage of monoclonal antibodies to treat prostate cancer, such as murine J591, 7E11 and human MDX-070 [2, 26]. However, none have reported tagging the AuNPs with antibodies specific for PSMA in order to attain a faster and enhanced selective treatment.

An interesting murine monoclonal antibody that has been found to have resonating advantages in prostate cancer treatments is D2B. D2B is specific for the extracellular epitope of human PSMA [27]. Binding of antibodies to PSMA induces endocytosis of the latter, thereby marking PSMA as a docking site for the delivery of therapeutic agents. This newly developed antibody by Guilio Fracasso and Marco Colombatti, was previously reported to improve intraoperative visualization and performing image guided resection of tumors [28]. Moreover, studies were done to prove how D2B embraces physiological conditions mainly by its efficient biodistribution, uptake by prostate cancer cells in vitro, and non-immunogenicity [29].

PSMA has been targeted by many monoclonal antibodies [30, 31] . However the various antibodies that target this antigen, differ in many aspects mainly in their mode of action, biological and clinical characteristics such as their stability, solubility, affinity, and specificity[29, 32]. D2B antibody is the novelest antibody that has shown to outperform existing PSMA monoclonal antibodies (mAb) in the context of the above mentioned characteristics. Taking the unique features and scope of D2B in prostate cancer therapy,

we reasoned that the perfectly tailored D2B-conjugated gold nanoparticles could be used to shuttle toxic payloads to PCa cells expressing the PSMA protein receptor. By this, we would achieve selectivity to prostate cancer cell death and our novel approach will prove to be an excellent and effective stratagem to successfully target and eradicate prostate tumors.

This study is the first to investigate the potential of conjugating a recently patented mouse monoclonal D2B antibody onto gold-citrate nanoparticles, and inspect its safe biological applications *in-vitro*, in order to provide an opportunity for a maximized anti-tumor effect of drug conjugates. We developed a new nanoplatform for the targeted delivery of chemotherapeutics, or for an enhanced photothermal therapy on the prostate cancer cells. A schematic representation highlighting this notion is depicted in figure 8.

Many anticancer drugs have poor water solubility, which hampers the ability of drugs to be administered via the intravenous route [33]. PSMA has been well established as a distinctive molecular target for prostate cancer treatment through immunotherapy or merely for tumor diagnosis since its expression is restricted to prostate cancer [34].

In the context of targeted prostate cancer treatment, the study at hand aimed to optimize the specificity to prostate cells by a recent manufactured antibody (D2B) that has shown enhanced PSMA binding (<https://patents.google.com/patent/WO2009130575A2/en>) and its conjugation to gold nanoparticles that are known to have optimum biodistribution *in-vivo* [35]. For this reason, the study was divided into two major goals, at first we wanted to test the effective binding of D2B to the gold nanoparticles that are coated with citrate by flow cytometry and western blot analysis, and then to assess their cytotoxicity by WST-1 and DNA fragmentation experiment.

Noteworthy, PSMA ligands are characteristically internalized into the cell upon ligand binding (antibodies or peptides), resulting in intracellular buildup and high levels of accumulation even dwells in metastatic cells [36].

In the present study, we report for the first time, the conjugation of a mouse monoclonal antibody (D2B), having superlative characteristics, with gold-citrate coated nanoparticles. The properties of AuNPs were characterized using Zeta potential measurements, UV-Vis spectroscopy, and dynamic light scattering (DLS) to confirm the binding of the D2B antibodies. To validate the safety of our synthesized gold nanoparticles, two cytotoxicity tests were applied to the prostate cancer cell line PC3-PSMA, namely WST-1 cell proliferation assay and DNA fragmentation method by gel electrophoresis. Furthermore, flow cytometry was implicated to confirm the D2B binding to the PSMA receptors on the prostatic cancer cells. Finally, Western blotting was done with the aim of assessing any reductions in the PSMA receptors and that might imply endocytic events due to AuNP-D2B binding. For the first time, we introduced a novel approach that targets prostate cancer cells with gold nanoparticles tagged to a specific antibody that recognizes an over-expressed PSMA protein receptor, and that is involved in the progression and metastasis of prostate cancer.

Our newly proposed method, will help us achieve a firm grip on prostate cancer treatment by shaping the fate of the nanotechnological approach that has been previously employed and rigging the therapeutic approach in our favor by enhancing prostate tumor targeting via the newly introduced AuNP-D2Bs. These biocompatible nanoparticles will mandate their future potential use as non-cytotoxic vehicles that can be loaded with therapeutics to effectively induce killing of prostate cancer.

II. Literature Review

1. Background on Prostate Cancer

Prostate cancer (PCa) is the cancer that affects the prostate gland in men. The prostate gland adheres firmly to the base of the bladder, and has a fundamental role in producing and secreting the prostate fluid that will mainly function to cushion and nourish the sperm with the seminal fluid along with other constituents such as enzymes and lipids [37].

It has become by far the most common malignancy in the face of the male population for it is the second most frequently diagnosed cancer in men worldwide [38].

Mutations in the genetic material lead to the growth of cancerous cells and these mutations may cause the prostate cells to grow in an abnormal and overwhelming manner, until a solid tumor develops [39]. Despite the fact that PCa is a slow growing cancer; however, it can become aggressive when metastasis occurs and spreads to other parts of the body. Prostate cancer metastasis mainly occurs to the bone, lymph nodes, and lungs [40]. Symptoms of advanced stages of the cancer include bone pain, often in the pelvis, blood in urine, trouble urinating [41].

In 2012, (the latest year for which worldwide PCa statistical information is available) [15] almost 1.1 million men were diagnosed with PCa in the world [42, 43] and reached 307,000 deaths during that year [44]. In the consecutive year there were 1.4 million cases of prostate cancer and 293,000 deaths worldwide in 2013 [45]. Notably, an overall gradual increase in prostate cancer incidence is observed with time [46]. The treatment of prostate cancer has been a subject of controversy for years. The development of therapies should be prioritized and targeted therapies have shown to serve as promising candidates in improving the efficacy of treatments and increasing the survival rate of patients [47].

For example, many studies have reported successful toxicity through targeted radioimmunotherapy (RIT) against PCa [48, 49].

1.1 Causes and Risk Factors of Prostate Cancer

The key elements causing prostate cancer remain unclear; however, some risk factors that increase its incidence, can be found in the literature. These mainly include: age, family history, and obesity[3]. In fact, prostate cancer incidence is largely correlated with age [50, 51]. Men that appreciably have the greatest risk are those above the age of 65 and the median age at death is 81 years [52].

The genetic history also seems to have a finger in augmenting the risk of developing prostate cancer [53, 54]. In one of the few studies done to study the effect of heredity on prostate cancer incidence (Gronberg *et al.*, 1996) showed that a positive family record for prostate cancer is associated with a doubled risk of incidence of the cancer in sons of the consequent generation. Therefore, they should regularly undergo appropriate screening measures for the disease. Other findings discerned by (Kolonel *et al.*, 2004) also indicate that exogenous factors such as food nutrition, pattern of sexual behavior, and alcohol consumption have all been discussed as being of etiological importance and affect the progression of prostate cancer [55].

1.2 Screening and Diagnosis of prostate cancer

Despite the substantive advances in prostate cancer detection, there remains significant uncertainty regarding current tumor diagnosis modalities [52]. Due to the insidious behavior of prostate cancer, early diagnosis remains problematic, and many patients are familiarized with the disease at metastatic stages during diagnosis [56].

PCa tumor is usually examined by digital rectal examination (DRE), prostate specific antigen (PSA) blood testing, and a prostate gland biopsy [57]. These tests are sometimes supplemented with conventional imaging techniques such as computer tomography (CT), bone scanning, or

magnetic resonance imaging (MRI) to detect changes in tissue morphology [50]. These methods can have a significant backlash to them, for example rectal examination detects the disease only at late stages and offers a wide array of inter-examiner variability, [58] and biopsy is an expensive and painful technique. Emerging evidence show that periodic testing for prostate-specific antigen (PSA) may reduce the likelihood of dying from prostate cancer [52]. PSA is a kallikrein-like serine protease produced by the epithelial cells of the prostate.

A PSA level of 4.0 ng/mL is considered a reasonable threshold for further evaluation; however, there is no true PSA cutoff point distinguishing cancer from non-cancer, [52] since recent studies have shown that some men with PSA levels below 4.0 ng/mL have prostate cancer and that many men with higher levels do not have prostate cancer [59]. Acknowledging this hurdle, patients are often counseled to go the extra mile of X-ray testing, trans rectal ultrasound examination, and cystoscopy to conclude the presence of prostate adenocarcinoma [47].

1.3 Current Treatments

Different treatments for prostate cancer can be employed and have existentially been witnessed to lead to variable undesirable side effects, [7] and thus it is undoubtedly essential to outline the different types of therapies that are currently available and decide accordingly. Typically, surgery and radiation therapy are two established protocols that are done when the cancer is local and confined to the prostate gland [50]. Radical prostatectomy, hormone, chemotherapeutic, and combination therapy options are ordinarily referred to when the disease is advanced (aggressive) and has spread to nearby tissue. Treatments at this time frame are only embarked to palliate the symptoms of the disease [7]. Overall, an active surveillance is acceptable for many men that are diagnosed with low-risk prostate cancer and are only treated when the tumor progresses with time, [60, 61] and more than 80 percent succumb to PCa after

metastasis occurs to the bone [62]. Moreover, the major demerit of chemotherapy lies in the non-selective uptake of drugs in healthy cells [63].

Given the complexity of the issue at hand, it is incumbent to seek different methods of treatment and all these findings warrant for further inspection of alternative therapeutic approaches. Lately, there has been an emerging body of evidence regarding the crucial and important role that NPs might play in the future for the diagnosis and, therapy as well, of prostate cancer [64].

2. Targeted Therapy and Nanotechnology

Nanotechnology has rapidly emerged in the field of medical imaging and targeted drug delivery [26]. The use of nanoparticles for example as both imaging and targeting agents may be coalesced to form a single entity capable of performing dual functions. The research on the development of such particles have keenly increased in the past couple of years [47]. Delivering chemotherapeutics to solid tumors effectively, or increasing their bioavailability remains a challenging problematic in current biomedical research; however, with the use of nanotechnology, this pitfall in our current approach for treatment would be eliminated and rectified [25]. This groundbreaking discovery is expected to greatly improve health care and medicine for it has already started to influence the way diseases, specifically cancer, is addressed, diagnosed, or even treated. The multifaceted world of nanosystems will be set on pedestal and will prove to be very promising for various medical applications [27].

The advantage that targeted therapy displays is the delivery of drugs specifically to cancer tissues and this feature allows it to be forefront relative to conventional chemotherapy regimens and offers an overall enhanced treatment since toxicity to healthy cells and adverse effects would be minimal [65, 66]. Overall, the benefit to patients undergoing chemotherapy is sufficiently low and is outweighed by the risks and harm stemming from treatment, tipping the balance in favor

of targeted alternative treatments and accentuating its importance [67]. Moreover, to overcome the mutability of cancer, it is critical to achieve an idealistic drug delivery vehicle that is characterized by long blood circulation and constitutes of clinically approved components to effectively combat the tumor within a short time frame [23]. In targeted therapy, having a uniquely overexpressed antigen on the tumor of interest, is of paramount importance since it reinforces the targeted delivery of the drugs and spares normal tissue. In prostate cancer, one overexpressed antigen is the prostate-specific membrane antigen (PSMA) [68, 69].

PSMA is a type II trans membrane glycoprotein (N-glycosylated) encoded by the folate hydrolase 1 (FOLH1) gene, also referred to as the glutamate carboxypeptidase II (GCPII) gene [70, 71].

This cell-surface protein (750 amino acids, 84 kDa) increases its expression progressively in higher-grade tumors [21]. Many researchers have substantiated that the role of PSMA lies in playing an agonistic role to integrins (e.g., $\alpha 2\beta 1, \alpha 3\beta 1$) and focal adhesion kinase signaling to promote endothelial cell activation and angiogenesis [72]. Moreover, PSMA has been proposed to regulate the expression of interleukin-6 and the chemokine CCL5 by activating the MAPK pathway; however, the exact role of PSMA and its implication in prostate cancer progression remains unclear.

In essence, it is reasonable to say that PSMA is an appealing and promising molecular target in prostate cancer management for a number of reasons, that basically involve its high levels of expression on the majority of prostate cancer cells and its limited expression on benign tissues, its proven *in vivo* safety and feasibility of targeting PSMA using antibodies and small molecules such as drugs and peptides, and finally having an internalization motif which provides

for internalization and concentration of agents [23]. Noteworthy, PSMA is constitutively internalized into the cell upon ligand induced binding, resulting in its intracellular recycling [23]. Monoclonal antibodies are useful entities when it comes to targeted drug delivery [73] and they have been used as imaging agents and to improve radiotherapy in tumors.

Interestingly, antibody-conjugated nanoparticles can have two biomedical applications: therapy and diagnosis. When it comes to therapy, the main application of antibody-conjugated nanoparticles is for the development of targeted drug delivery along with enhanced tissue repair. In diagnosis, however, the applications can be divided according to the nature of the experimentation which is either *in vivo* or *in vitro* and these include magnetic resonance imaging (MRI), sensing, cell sorting, bioseparation, enzyme immobilization, immunoassays, transfection (gene delivery), purification, and so forth [74]. Antibodies have been known for their robustness and flexibility and have been widely used in pharmaceutical, biotechnological, and industrial applications. Antibodies hold a great potential in treating a wide array of diseases such as cancer, asthma, immune and infectious diseases and interest in promoting antibodies for further investigation and the eagerness to use them as therapeutic molecules have immensely increased and this is due to the ability that antibodies can bind and recognize with high specificity to infinite molecules, and hence allowing targeted therapy while avoiding undesirable side effects [75]. Many studies have been done to show that targeted nanoparticles have a higher tumor uptake and greater efficacy than non-targeted nanoparticles. A comprehensive survey of the literature from the past 10 years indicated that only 0.7% (median) of the injected dose of nanoparticles was delivered to the tumor. Active targeting strategies on the other hand, had a higher delivery efficiency of 0.9% than passive targeting (0.6%) approaches. Other advantages of antibody-mediated targeting are the possibility of using multiple antibodies to overcome

tumor heterogeneity and avoid drug efflux to overcome multidrug resistance [76]. Overall, the utilization of nanotechnology is the need of hour against the war on cancer.

In the following sections, we describe major studies published regarding different types of nanoparticles and their applications in the treatment and diagnosis of prostate cancer. More than seven thousand articles have been peer-reviewed and added to the literature database since 1998. A focus on gold nanoparticles that were applied for prostate in the past two decades, from 1998 till 2018, was done. PubMed, Science Direct, PLOS One, AACR, Nanomedicine, Springer, and Nature were used as search engine databases for studies including “Antibody-coated gold nanoparticles in prostate therapy” and “PSMA targeted gold nanoparticles” along with “Gold Nanoparticle applications for prostate cancer”. The search was restricted to the English language and the type of publication was set to “Journal”. Sixty percent of the studies on gold applications involved other types of cancers such as breast, colorectal, and lung cancers etc.... Another twenty percent contained an adverse gamut of the broad applications of different types of nanoparticles in cancer therapy that were not restricted to gold. The remaining twenty percent was collected as EndNote databases and screened for duplicates. Thus, our main goal was to provide an updated review incorporating the latest 20% of articles that match our search criteria. Despite the existence of a recent literature review “Theranostic Nanoparticle Applications: A focus on Prostate and Breast Cancer” by (Elgvist et al., 2017), we sought to further delineate and illumine on all the studies done on prostate cancer using gold nanoparticles as the coverage was narrowly reported. Almost 20 articles were not mentioned by Elgvist and consequently added to our review, as depicted in table 1.

2.1 Theranostic NP applications for Prostate Cancer

The use of nanoparticles that are generally less than 100nm in size [77], has increased exponentially in recent years. The key benefits of nanotherapy can be disentangled into two major objectives with the first being, maximized drug loading capacity, and the latter would be increased tumor uptake by ameliorated drug circulation and lessened risk of undesirable toxic effects to nearby healthy tissue [78, 79]. This notion can be exemplified and put into perspective by the ample studies done on prostate cancer using nanomaterials in an attempt at ridding the tumor or enhancing diagnosis.

2.1.1 Iron Oxide Nanoparticles

Iron oxide particles have magnetic properties that enable their use in several magnetic resonance technology-based biomedical applications and superparamagnetic nanoparticles (SPIONs) with a diameter of 20 nm have mostly been adopted for such applications.

To prevent aggregation of the particles caused by van der Waals and hydrophobic interactions, polyethylene glycol (PEG) molecules are added to its surface, thereby hindering aggregation but also masking the NP from the immune recognition [80]. Silica coatings are also used with iron oxide nanoparticles to enhance light absorption in imaging applications. Among the various iron oxide NP studies done on prostate [81], Zhu et al. illustrated the significantly enhanced magnetic resonance imaging (MRI) and PSMA targeting achieved by the innovative iron oxide nanoparticles. Moreover, results showed specific uptake of the particles by the PSMA expressing cells. They concluded that prostate PSMA-targeting by SPIONs serves as a strong argument for the theranostic NP-based platform [47].

Sterenczak *et al.*, 2012, also demonstrated enhanced *in-vivo* prostate tumor MRI imaging and monitoring by SPIONs, and *in-vitro* as well when applied to canine prostate cell line CT1258 [82]. In a study done by Agemy *et al.* 2010, the nanoparticle-induced vascular blockade in human prostate cancer was investigated with the use of iron oxide nanoworms in prostate tumor blood vessels. Their aim was to occlude tumor vasculature to induce necrosis. The results showed that targeting the iron oxide nanoworms with a peptide that recognizes fibrin-fibronectin complexes result in the accumulation of the nanoparticles in the tumor vessels and they induce additional local clotting; however, no significant inhibition of tumor growth was obtained [83].

2.1.2 Gadolinium, Manganese, Silver, and Platinum

Gadolinium (Gd^{3+}) is most commonly used to date as a contrast enhancing agent for magnetic resonance imaging (MRI) since areas with enriched Gd^{3+} exhibit increase signal intensity and have the ability to cross the blood brain barrier and permeate brain tumor imaging [84-86]. However, considerable research efforts have focused on developing cell-permeable contrast agents since Gd^{3+} is restricted to the extracellular environment [85]. In the case of gadolinium, they can be loaded onto nanostructures to increase the efficiency of cellular uptake and endow other prospects such as targeted therapy [87]. For example (Cui *et. al.*, 2017) reported that bombesin (BBN) modified gadolinium oxide nanoprobe could be targeted to gastrin-releasing peptide (GRP) over-expressed receptors in prostate cancer cells to enhance diagnosis and antitumor drug delivery in the future [84].

On the other hand, the use of manganese (Mn^{2+}) as a contrast agent in nanoprobe, has just started to accelerate. Only one such article was found to depict this topic, the study done by (Gao *et. al.*, 2012), reported the use of manganese doped quantum dots for prostate cancer imaging [88]. Remarkably efficacious results were achieved for high-specificity cell imaging.

Silver nanoparticles (AgNPs) have not been intensely employed for prostate cancer as gold nanoparticles, in fact they have been broadly investigated as antimicrobial agents [89-91]. Among the scarce studies that have focused on its anti-tumor effects on prostate, was a study done by (Firdhouse et. al., 2013) that showed AgNPs exert cytotoxic effects on the prostate cancer line (PC3) by inhibiting proliferation in a concentration dependent manner and inducing apoptosis [92]. Coherent to this notion, (Mohammadzadeh, 2012) revealed that when AgNPs accumulate in the tumor environment they deplete antioxidants by binding to them. Consequently, reactive oxygen species (ROS) prevail since they are not being neutralized and the cell subsequently initiates programmed cell death [93]. Wang et al. on the other hand, developed mesoporous silica nanoparticles that are hybridized with silver (Ag), in order to test for the prostate specific antigen (PSA) in the human serum. [94] The AgNPs demonstrated enhanced sensitivity for PSA detection and in a much simpler manner than conventional PSA detection methods that include ELISA and several other assays. In addition, in an in vitro study, AgNPs were synthesized from a Chinese herbal *Cornus officinal* plant and an aqueous extract of Shanzhuyu was prepared from the herb, to induce cytotoxicity to PC3 cells [95]. The AgNPs exhibited cytotoxicity against the PC-3 cells with an LC50 value of 25.54 µg/mL in 48 hrs.

In regard to Platinum-based NPs (PtNPs) for prostate cancer applications encompassing diagnosis and treatment a limited number of publications have been reported [96, 97]. PtNPs could be endowed unique properties such as size and morphology and offer great potential in many fields. Zhang and colleagues reported the use of PtNPs conjugated to an anti-PSA antibody for a sensitive determination of PSA in the serum [98]. Spain et al. proposed a facile method also incorporating PtNPs that are conjugated to a recombinant scFv antibody for the detection of PSA during PCa diagnosis. Results showed that PSA at picomolar concentrations could be detected

[99]. Taylor *et. al.*, (2012) used an anti-PSMA antibody (J591) conjugated to superparamagnetic iron platinum nanoparticles (SIPPs) that is encapsulated by the chemotherapeutic drug paclitaxel, on prostate cancer cell line C4-2. Results showed MRI contrast enhancement due to the enhanced permeability and retention effect and site specific drug delivery in *in vivo* experiments [100].

2.1.3 Quantum Dots

The semiconductor nanocrystals known as quantum dots (QDs) have greatly raised attention because of their unique optical properties (size dependent electron excitation) and varied utilization in biological and biomedical studies [101]. They are mainly fabricated from combinations of heavy metals such as CdSe, CdS, PbS ZnS [102]. Traditional fluorescent labels fall short of providing long-term stability and simultaneous detection of multiple signals when juxtaposed to QD. In fact, they have been shown to hold great promise in applications such as cellular labelling, deep-tissue imaging, and as efficient fluorophores. However, despite recent progress made, great concern has been elevated to their heavy metal involvement. These heavy metals (Zn,Pb,Cd) can be potent toxins, neurotoxins and teratogens depending on dosage and complexation, accumulating in and damaging the liver and nervous system [103]. For this reason, scientists have been prompted to pursue alternatives such as silica based Cornell dots (C dots) [104]. These C dots can be further coated with a common polymer such as polyethylene glycol (PEG) in order to increase their circulation in the blood by decreasing the kidney clearance and permitting their conjugation to monoclonal antibodies (mAbs) that are site specific for cancer cell receptors along with anticancer drugs [105].

PCa applications involving QDs have been lightly conveyed with the majority dealing with diagnosis and imaging rather than therapy [106-108]. In a study done by (Malekzad *et. al.*, 2017),

the use of graphene quantum dots complexed with gold nanoparticles (GQDs/AuNP) and garnished with anti-PSA antibodies, for dual signal amplification and highly sensitive PSA detection, was reported [109]. Singh *et al.*, 2012, stipulated that cadmium sulfide (CdS) quantum dots induce ROS-mediated apoptotic cell death in prostate cancer LNCaP cells, increase p53 and Bax protein expression [101].

2.1.4 Liposomes

Liposomes are composed of a phospholipid bilayer that is arranged into a spherical vesicle having an aqueous core that enables it to encapsulate both hydrophilic and lipophilic molecules [110, 111]. These biodegradable and nontoxic particles have shown to promote the enhanced retention and permeability (EPR) effect at the tumor site by enhancing tumor uptake [112, 113].

Among the organic NPs liposomes are the simplest forms of vesicles and they are mostly used as carrier especially for passive targeting [114]. However, a striking contradiction exist when skimming through the literature on liposomes since some studies have reported that liposomes have some major drawbacks such as easy oxidation, hydrolysis, unstable structure, and high leakage of the drugs from the carriers that lead to its limited usage as an ideal candidate for the transport of actively targeted nanocarriers. In general, organic nanoparticles are less stable at high temperatures [115].

Rajesh and co-authors have published experimental results that portray liposomes as efficient nano-carriers. To enhance the targeted delivery of their anticancer agent Rajesh *et al.*, used curcumin loaded liposomes, with sizes ranging from 100-150 nm, for drug delivery to prostate cancer cells and coated them with anti-PSMA antibody. Treatment of the LNCap and C4-2B cell lines resulted in 70-80% reduction in proliferation, using MTT assay. While curcumin alone on

the other hand needed a 10 fold higher concentration to exert the same cytotoxic effects (>50 μM) [116].

Based on the pioneering work of Yeh *et al.*, active liposomal targeting was also made possible by the SP204 peptide-conjugated liposomal NPs that were conjugated to doxorubicin (chemotherapeutic drug that intercalates DNA) and vinorelbine, hence were significantly capable of inhibiting PCa growth as well [117].

Sauvage *et al.*, customized liposomes containing the molecular chaperone heat shock protein 90 (Hsp90) inhibitor 6BrCaQ for prostate cancer cells. The Hsp90 plays a key role in the maturation of proteins implicated in oncogenic pathways. Their results showed that the NPs induced apoptosis and cell cycle arrest in PC3 cells [118]. They have also shown to synergize with DOX and slow down cell migration. Few studies can be found for the “active” targeting of liposomes to prostate cancer cells and some of which include studies done by Xiang *et al.*, and Banerjee *et al.*, for example, Xiang attempted at targeting the liposomes to prostate by tagging them to a folate moiety that eventually binds over-expressed PSMA receptors in the cancer cells. The liposomes were also loaded with siRNA that showed to decrease polo-like kinase 1 (PLK-1) expression and augment apoptosis [119]. Banerjee *et al.* took a similar approach for active targeting of DU-145 human prostate adenocarcinoma cell line; however, the liposomes were tagged to an anisamide ligand that targets sigma receptors and DOX was used as the anti-cancer agent which was encapsulated in the vesicles. The anisamide-conjugated liposomal DOX showed significantly higher toxicity to DU-145 cells than non-targeted liposomal DOX, the IC₅₀ being 1.8 μM and 14 μM , respectively [20].

2.2 Gold Nanoparticles (AuNPs)

Narrowing down on the vast and innumerable drug delivery vehicles that have been employed, gold nanoparticles have been greatly explored due to their enhanced biodistribution and their potential to accommodate large payloads that have rendered them appealing to scientists [120]. The use of gold nanoparticles is assured to have a crucial impact in the field of nanotechnology and in shaping the future of targeted cancer therapy due to their inherent capability to exert therapeutic effects and to be designed to match the sizes of tumor vasculature in order to have optimal results by incorporating payloads with minimum leakage away from target sites [121]. Among the prostate targeted treatments that used gold nanoparticles, was a study done by Shukla *et al.* (2012), that applied tumor specific epigallocatechin-gallate (EGCg) functionalized radioactive gold nanoparticles (EGC-tagged AuNPs) to target overexpressed laminin receptors on the prostate cells and induce cytotoxic effects resulting from the attached phytochemical extracted from green tea, when delivered intratumorally; hence, circumventing transport barriers and resulting in targeted delivery of therapeutic payloads [121].

Another promising *in-vivo* study showed up to 80 percent tumor reduction when magniferin radioactive AuNPs, having laminin receptor specificity, were applied in the prostate tumor [15]. Guo *et al.* for example took advantage of small-interference RNA (siRNA) conjugated to AuNPs to knock down gene expression in prostate cancer cells (PC-3 and LNCaP). Their results offer potential applications of their transferrin and folate receptor ligands conjugated to AuNPs in prostate cancer treatment [122].

Conversely Oh *et al.* (2015) showed that efficient PCa killing was feasible when photothermal therapy was applied on AuNP clusters by low light irradiation that caused local heating and selective killing of the PC-3 targeted cells [123].

Lu *et al.* (2017) revealed that chrysophanol gold nanoparticle in mice model showed high bioavailability with sustained releasing properties compared to the free chrysophanol. Chrysophanol extracts from *Rheum* genus plants has been suggested to alter major signaling pathways leading to cell death in different types of cancer cells [124].

Similarly, Tsai *et al.* (2016) used a green tea natural extract epigallocatechin gallate (EGCG) on metastasized human prostate cancer cells (PC-3), to override the obstacles that systemic anticancer drug delivery conveys mainly through poor targeting and intracellular uptake. In their study, the chemotherapeutic drug Doxorubicin (DOX) was successfully complexed to the EGCG-functionalized AuNPs (EGCG- AuNPs). MTT assays and Laser Scanning Microscopy results showed that cell proliferation of the PC-3 cells was inhibited concomitantly with enhanced cellular uptake of DOX [125].

Rodriguez *et al.* (2018) outlined a porous silicon tethered to 100 nm gold nanoparticles (PSi-GNP) based platform as biosensors for enhanced PSA detection. The gold nanoparticles relayed the added value of enhanced conductivity in the sandwich bioassay [126]. Barbosa *et al.* (2017) unraveled a new method towards achieving an optimum one-step quantitation of PSA using silver-enhanced gold nanoparticles conjugated to anti-PSA antibodies together with carbon nanoparticles [127]. They aimed at promoting a novel optical detection method using a microcapillary film (MCF) as an immunoassay platform. PSA was successfully quantified in a cost effective method using the silver-enhanced gold nanoparticles, presenting a dynamic range of 10 to 100 ng/ml of PSA. However, the authors reported that optimization and refinement is still needed to achieve a more sensitive quantification. One similar approach that was anticipated for sensitive PSA detection, was a study done by Pal *et al.* (2017) in which gold nanoparticles supported with graphene oxide (Au-GrO) and attached to anti-PSA antibodies were used as a

novel biosensor that was applied to human prostate epithelial cells, RWPE-1. The immunosensor resulted in a highly selective and stable model, having a low PSA detection limit of 0.24 fg/mL [128]. Suresh *et al.*, (2018) also applied an identical method, however gold nanoparticles that are coated with a chitosan polymer were used instead, to establish binding to the anti-PSA antibodies [129]. Vural *et al.* (2018) on the other hand, proposed a method for PSA detection in blood serum samples, that involved a self-assembled peptide nanotube (PNT), gold nanoparticle (AuNP) and polyaniline (PANI) composite (PANI/AuNP-PNT) that was used to modify a pencil graphite electrode (PGE). Anti-PSA (Ab1) was immobilized on the modified electrode (PANI/AuNP-PNT/PGE) to capture PSA and horseradish peroxidase (HRP) labeled anti-PSA (HRP-Ab2) was used as a tracer antibody. The practicality of the novel method was compared to enzyme-linked immunosorbent assay (ELISA) and compatible results were obtained and the limit of detection was found out to be 0.68 ng/mL [130]. Butterworth *et al.*, (2016) performed a preclinical evaluation of dithiolated diethylenetriamine pentaacetic acid (DTDTPA) conjugated AuNPs (Au@DTDTPA) for both CT-contrast enhancement and radiotherapy in prostate cancer [131]. The gold-DTDTPA nanoparticles showed that they are capable of acting as efficient theranostic agents in prostate cancer by inducing cytotoxicity in the PC3, DU 145, and PNT2-C2 cells after a 24hr exposure to the NPs. Moreover, the Au@DTDTPA gave rise to a 10 % CT imaging enhancement. The inert trait of gold nanoparticles was also exploited as a powerful means for enhanced imaging for prostate cancer by Harmsen *et al.*, (2017). In his study 60 nm gold nanoparticles were encapsulated with a silica shell to achieve a promising contrast agent for in vivo cancer imaging. The authors also managed to introduce several applications of these nanoprobables for biomedical research such as intraoperative cancer imaging and a straightforward delineation of cancer without the need for a specific biomarker targeting [132]. Sattarahmady *et*

al. (2017) gave insight on a novel method for PSA detection however using a round hairbrush-like gold nanostructure conjugated to an aptamer. The fabricated aptamer biosensor was capable of detecting PSA with a minimum limit value of 50 pg/mL [133]. In a very recent study by Srivastava *et al.* (2018) the authors also shed light on newly instrumented biosensor composed of graphene quantum dots and gold nanorods (GQDs-AuNRs). Their research constituted of a comparative study between an immunosensor (anti-PSA) or an aptasensor (aptamer) bound to the nanoparticles, to efficiently quantitate and detect PSA levels. The performance of both sensors showed comparable results with an almost same limit of detection (LOD) of 0.14 ng/mL. The aptasensor however did have some advantages over the immunosensor in terms of stability, simplicity, and cost effectiveness [134]. Huang *et al.* 2005 showed that using a single domain antigen-binding fragment, such as anti-PSA VHH camel antibody (cAbPSA-N7), derived from dromedary heavy-chain antibody, and applying it to a colloidal streptavidin coated gold nanoparticle sandwich assay for PSA detection was found to be a very promising method as well and enabled the detection of PSA levels as low as 1 ng/ml [135].

Mayle *et al.* (2016) worked on engineering an A11 minibody-conjugated to a gold nanoshell for prostate stem cell antigen (PSCA) in order to facilitate targeted photothermal therapy on PSCA-transfected 22Rv1 prostate cancer cells. Results showed significant laser-induced, localized killing of prostate cancer cells *in vitro* by exhibiting greater efficacy as a photothermal therapy agent compared to nontargeted gold nanoshells [136]. A real breakthrough arose when Kim *et al.* (2017) managed to demonstrate the selective uptake of epidermal growth factor-conjugated gold nanoparticle (EGF-GNP) and how it facilitates non-thermal plasma (NTP)-mediated cell death in prostate DU 145 cells along with other cell lines over-expressing the epidermal growth factor receptor (EGFR). Treatment with EGF-conjugated GNP complex, followed by NTP irradiation

showed selective apoptosis of cells that have undergone receptor mediated endocytosis. These results suggest that EGF-conjugated GNP functions as an important adjuvant which gives target specificity in applications of conventional plasma therapy [137].

In an interesting study managed by Lechtman *et al.* (2017), the authors came out with a conclusive finding that there is an interplay between the gold nanoparticle sub-cellular localization, size, and the photon energy for radiosensitization in PC3 prostate cancer cells [138]. Khoo *et al.*, (2017) studied the effect of radiosensitization of prostate cancers *in-vitro* and *in-vivo*, to X-rays using actively targeted goserelin-conjugated gold nanorods (gGNRs) [139]. The study showed that treatment of prostate cancer cells with goserelin-conjugated gold nanorods (gGNRs) promotes gonadotropin releasing hormone receptor-mediated internalization and enhances radiosensitivity. The *in-vivo* results showed that gGNR treatment along with x-ray irradiation is considerably more effective than radiation treatment alone ($p < 0.0005$) hence, resulting in a striking reduction in tumor volume that was 50% smaller after only 2 months of treatment. Their results provided strong evidence for the feasibility of tumor-specific prostate brachytherapy with gGNRs. However, Kasten *et.al.* 2013 highlighted on the feasibility of efficiently targeting prostate cancer cells with PSMA inhibitor (CTT54)-guided gold nanoparticles. The PSMA-targeted AuNPs exhibited significantly higher and selective binding to LNCaP cells compared to control non-targeted AuNPs in a time-dependent manner [140]. Through modulating the AuNPs' shape, size, or surface characteristics it is possible to fine-tune their properties in order to maximize their applicability as a tool for cancer diagnosis, photothermal therapy, radiotherapy, and targeted gene therapy [141].

In brief, the significance of AuNPs boils down to the versatile platform they offer through the afore mentioned modifications, which allows them to be conceived as potentially capable

contenders in the area of active tumor targeting and imaging. Taking the unique features of AuNP into consideration, we sought to develop a nano pharmaceutical that can target PCa with therapeutic combinations that target the PSMA receptor. Recognizing the growing global prostate cancer crisis, a smart vision is needed to implement nanoparticles as drug carriers.

Our approach is envisioned to play a pivotal role in targeted prostate therapy and will provide unprecedented results that will set the railway tracks for further future developments in prostate treatment and new avenues will arise as our ability to manipulate these materials improves. Vulnerability towards prostate cancer will increase owing to the unique properties that this prominent nanocarrier exploits.

III. Materials and Methods

1. Chemicals

Purified H₂O (resistivity $\approx 18.2 \text{ M}\Omega \text{ cm}$) was used as a solvent. All glassware was cleaned with aqua regia (3 parts of concentrated HCl and 1 part of concentrated HNO₃), rinsed with distilled water, ethanol, and acetone and oven-dried before use. Tetrachloroauric acid trihydrate

(HAuCl₄, 3H₂O), sodium citrate dihydrate (C₆H₅Na₃O₇·2H₂O) and sodium hydroxide were purchased from Sigma Aldrich. WST-1 cell proliferation reagent was purchased from Roche. All chemicals were used as received without further purification.

2. Synthesis of Gold Citrate (AuNP-Citrate) Nanoparticles

- A. Synthesis of AuNPs-Citrate :** To a 100 mL round flask containing 48 mL of deionized water at 95 °C, 100 µL of NaOH (0.1 M) and 0.961 mL HAuCl₄ (13 mM) were added under stirring, followed by the fast injection of 0.625 mL of sodium citrate (0.1 M). The colour of the solution changed from pale yellow to colorless within about 2 mins, then to gray after about 5 mins, then shifted to clear red that deepened with time to deep red wine (~ 30 mins). The solution was kept under stirring for 30 mins after the color was stabilized (deep wine red). The obtained nanoparticles have a hydrodynamic diameter of about 25 nm (size by number from DLS measurement) and a zeta potential of -46 ± 1 mV.
- B. Conjugation Protocol:** To a 50 mL beaker containing 10 mL of the AuNPs-Citrate pristine solution in ice bath, 400 µL of D2B solution (0.099 mg/mL) was added dropwise. The colour of the solution changed gradually from deep red wine to pink violet, the stirring was stopped after about 1 hour of addition. UV-Vis and DLS analysis were performed to confirm the D2B attachment onto AuNPs surface.

3. UV-Visible Spectroscopy analysis

Optical spectra were obtained on a UV/Vis Analytikjena SPECORD® 250 PLUS spectrophotometer (300–900-nm range, 0.5 nm resolution).

4. Dynamic Light Scattering and Zeta Potential measurements

The size distribution and surface charge (zeta potential) of the AuNPs colloidal solutions were determined by dynamic light scattering (DLS) with the Malvern Zetasizer Nano-ZS (model ZEN3600; Malvern Instruments Inc., Westborough, MA, USA) using the default NIBS 173° back scattering technique. The model used in the fitting procedure was based on Mark Houwisk parameters. Data was fitted using the cumulative fit given by the suppliers. Measurements were performed on the pristine solutions of AuNPs (~50 µg/mL) using disposable folded capillary cuvettes at 25 °C. Triplicates of each sample have been made for result comparison efficiency.

5. Cell Culture

Prostate cancer cells over-expressing the PSMA receptor (PC3-PSMA) were kindly provided by Prof. Giulio Fraccasso. The cell line was cultured in RPMI 1640 supplemented with 10% fetal bovine serum and antibiotics (100 U/mL penicillin and 100 µg/mL streptomycin) in a humidified atmosphere containing 5% CO₂ at 37°C. The cells were grown in a monolayer (70–80% confluence) before being incubated with various concentrations of the nanoparticles. The cells were detached using trypsin and split every 3 days at a ratio of 1: 9. Before plating, 10 µL of the cells were mixed with 10 µL of trypan blue and counted using a hemocytometer to check the cell viability.

6. WST-1 Cell Proliferation Assay

When PC3-PSMA cells were cultured to the log phase they were seeded in 96-well plates at a seeding density of 5×10^4 cells/ml and incubated overnight. In order to treat the cells, the whole media in each well was discarded and replaced with increasing concentrations of nanoparticles alone or conjugated to D2B antibody (NP= 20.75µg/ml, C1=12.45µg/ml, C2=

6.22 μ g/ml, C3=3.11, C4=1.04 μ g/ml μ g/ml). As a control, gold nanoparticles were resuspended with deionized water and serum free media to reach the final concentration needed and a final volume of 200 μ L/well. The cells were incubated for 4 hours in a CO₂ incubator (5% CO₂). The results were read on a “MultiGo-Scan” ELISA reader. All wells were treated with 10 μ L of WST 1 reagent (Roche), incubated for 2 hrs and the absorbance was read at 450 nm.

7. DNA Fragmentation

In a 24 flat-well plate, PC3-PSMA cells were seeded at a seeding density of 2x10⁵ cells/ml. The cells were then treated with the desired concentration of AuNP or AuNP-D2B for 4 hours. After treatment, cells were trypsinized, resuspended in RPMI, and collected in eppendorf tubes for centrifugation at 1500 rpm for 5 min. Cells were treated with 75 μ l of lysis buffer for 25 min on ice (4 °C) and then centrifuged for 27 min at high speed. Phenol Chloroform (1:1) was used to extract the DNA with vigorous vortexing followed by centrifugation at 14800 rpm for 1 min at RT and the top aqueous phase was transferred to a fresh tube. The DNA was then pelleted with 5M Sodium acetate, 2ml ethanol and was spun down for 15 min at top speed. The pellet was resuspended in 60 μ l of deionized water-RNase solution (0.4 mL water + 5 μ l of RNase) and DNA quantity and quality was assessed by Nanodrop. After checking the concentration, the samples were diluted to a final concentration of 1 μ g/ μ L and mixed with 5 μ l loading buffer.

The samples were run on a 1% agarose gel for 50 minutes at 65V. After that, the DNA bands were viewed on a UV-transilluminator.

8. Flow Cytometry

PC3-PSMA cells were seeded at a density of 2 x 10⁵ cells/mL in a 24-well plate and were left to grow overnight. The cells were then treated with the desired concentration (0, 6, 12, and

20 µg/ml) of nanoparticles conjugated to D2B in triplicates for 4 hours. Cells were then trypsinized for 1 min with 100 µl trypsin to dislodge the cells and were resuspended with 200 µl of RPMI media. We then transferred the cells to separate eppendorfs and centrifuged for 5 min at 1500 rpm. The pellet was resuspended with 900µl PBS and 100µL of 4% PFA and transferred to Flow cytometry cuvettes. 2 µL of FITC was added to each vial and were left to incubate in the dark for 1 hr with gentle shaking every 15 min. The samples were read using a PARTEC Cube 8 flow cytometer and the data was extracted and further analyzed using the FlowJo software. Finally, data measurements were normalized using a basic statistical formula as depicted below where the normalized value $z = (x_i - \min(x))/(\max(x) - \min(x))$, where $\min(x)$ corresponds to lowest value of the control data set and $\max(x)$ corresponds to the highest value of the highest AuNP-D2B concentration data set, and (x_i) stands for the value to be normalized. The results were plotted using EXCEL [141].

9. Western Blot

PC3-PSMA or PC3-WT cells were plated and cultured to reach confluence in a 75cm³ culture flask (4×10^6), then treated with AuNP-D2B or D2B alone (20 µg/mL) for 4 hrs at 37 °C. The cells were then trypsinized and centrifuged at 1500 rpm at 4 °C. Cell lysate was then prepared by adding lysis buffer (400 µL) to the cells and were left on ice for 30 min. The cells were then centrifuged at 16,000 g for 20min at 4 °C. The supernatant was transferred to new eppendorfs and mixed with equal volumes of 1× Laemmli buffer. The samples were then boiled at 100 °C in a heating block for 5 min. 20 µL of the samples from each concentration were loaded on a 10% SDS-PAGE gel and were left to run at 200 V for 75 min. Protein were then transferred to a nitrocellulose membrane at 30 V overnight. The membrane was then blocked with 5% dry skim milk in TBST containing 0.05% Tween-20 for 1 h at room temperature with

shaking. The membrane was then incubated with anti-actin monoclonal mouse antibodies (1:5000) at 4°C overnight with gentle shaking. After washing the membranes, with 1× TBS (0.5% Tween 20) for 15 min, they were incubated with the secondary antibody (anti-mouse IgG HRP-conjugated secondary antibody) at a concentration of 1:5000 for 1hr at room temperature. The membrane was then washed and developed using Western blotting-enhanced chemiluminescent reagent (ECL Detection Kit), and pictures were taken using a ChemiDoc machine.

10. Statistical Analysis

All the experiments were carried out in triplicate, and each experiment was repeated three times. The results are reported as the mean \pm standard deviation. The data was analyzed using one-way ANOVA. The level of significance upon comparing the control versus treatment was set at $p < 0.05$.

IV. Results

1. Synthesis and Characterization of AuNPs-D2B.

Addition of D2B to AuNPs-citrate colloidal solution caused a red shift (higher wavelength) by about 15 nm in the UV-Vis spectra as shown in Figure 1. This change in color might be due to the change in the refractive index around the AuNPs as a result to the attachment of D2B [142]. Furthermore, dynamic light scattering (DLS) showed an increase in the AuNPs size from ~25 to about ~ 63 nm (size distribution by number) as a confirmation of the successful conjugation of AuNPs-Citrate with D2B (Figure 2). On the other hand, Zeta potential measurements revealed an increase from ~ -45 mV for AuNPs-Citrate to -23 mV (data not shown).

2. WST-1 Cell Proliferation Assay

To investigate whether our synthesized D2B-AuNPs and AuNPs alone affect the proliferation profile of the prostate cancer cells, a WST-1 reagent was used. The tetrazolium salt, WST-1, is cleaved to a soluble formazan by a cellular mechanism that occurs primarily at the cell surface. This reduction is largely dependent on the glycolytic production of NAD(P)H in viable cells. The results in figure 3 and 4 support the non-cytotoxic effects of AuNP-D2B and AuNPs, since the percent viability remained above 80 % for all the concentrations used and even at the highest concentration of Nanoparticles the percent viability was comparable to the control with a 98.4 % and 90 % viability for the AuNPs alone and AuNP-D2B, respectively.

3. DNA Fragmentation

To evaluate the biosafety and cytotoxic effects of our customized D2B-AuNPs, genomic DNA was extracted after treating the PC3-PSMA cells with various concentrations of the NPs ranging between 0 and 20 µg/mL. DNA fragmentation analysis was profiled on a 1 % agarose

gel electrophoresis in search for cleaved DNA that is a hallmark of apoptotic cells. The genome remained intact with all the concentrations used as observed by the DNA bands above the 1kb DNA ladder and non-fragmentation was observed.

4. Flow Cytometry Analysis

Next, we investigated the binding of AuNP-D2B to the overexpressed PSMA ligand on the PC3 cells. After a 4 hr cell treatment with the various concentrations of the D2B conjugated AuNPs, flow cytometry was done using a goat monoclonal anti-D2B FITC secondary antibody to track the efficiency of D2B binding. The histogram results revealed an evident shift and increase in FITC fluorescence only upon treating the cells with the highest concentration of AuNP-D2B (20 $\mu\text{g}/\text{mL}$). Remarkably, low concentrations ranging between 6 to 12 $\mu\text{g}/\text{mL}$ showed a similar background signal as untreated cells (control).

On the other hand, the increase in the mean fluorescence intensity (FL1), at lower concentrations was observed with the histogram analysis of fluorescence from the three separate trials in figure 7. The results show a significant mean fluorescence intensity increase of 30 and 50 when 12 and 20 $\mu\text{g}/\text{mL}$ of AuNP-D2B were added, respectively, while the 6 $\mu\text{g}/\text{mL}$ of treated cells showed a non-significant intensity of about 20, when compared to the control. This reveals that the FITC fluorescence intensity increased as the concentration of AuNP-D2B increased.

Furthermore, a normalized mean fluorescence intensity graph was conducted in an attempt to better analyze our results. Our data set was normalized using the formula described in the materials and method section, for all the concentrations used.

5. Western Blot

Western blot analysis was employed to assess PSMA specificity to the D2Bs, and for this reason PC3-WT cells lacking PSMA were used at this point. Moreover, we aimed to compare the resulting band obtained from either using the primary D2B alone or conjugated to AuNPs at a concentration of 20 μ g/mL, in order to be able to use AuNP-D2B alone in future experiments. Results show that no band was observed for the PC3-WT cells (PSMA⁻) and two very similar bands were observed for both lanes of the PC3-PSMA cells.

V. Discussion

In this study, gold nanoparticles were synthesized in water at near boiling point through the chemical reduction of gold precursor ($\text{HAuCl}_4 \cdot 3\text{H}_2\text{O}$). In order to avoid uncontrolled increase in the size and to achieve a high stability of the resulting nanoparticles, citrate was added during the synthesis. The added citrate ligand adsorbs onto the growing AuNPs surfaces and therefore allowing their final size stabilization and surface charge modification. Specifically speaking, the citrate acts as an electrostatic stabilizing agent by preventing Van der Waals interactions that lead to the aggregation of nanoparticles and increases its shelf life by. This electrostatic stabilization, arises particularly from the mutual repulsion of neighboring AuNPs, resulting from the negative charge of the citrate layer [143].

The binding of the antibodies onto the AuNPs was feasible due to an ionic-covalent interaction that exists between the thiol group in the cysteine amino-acid and the negatively charged citrate molecules on the AuNPs that causes their reduction. Moreover, they have shown to have a high affinity to the surface of nanoparticles. Apart from thiols, amine groups in proteins have also shown to be protonated in our slightly acidic solution of the AuNPs (6.23), which also favors their binding onto the negatively charged particles causing a charge-charge interaction (ionic) [144]. A representative image is seen in figure 10.

The obtained AuNPs prepared in this study were characterized by UV-Visible absorption spectroscopy. To achieve successful conjugation and high affinity binding of D2B to the AuNPs, the mercapto group (SH) in cysteine of the D2B was used and the particles were characterized using ultraviolet-visible spectroscopy (UV-Vis), dynamic light scattering (DLS) and Zeta potential measurements.

The physicochemical properties, obtained from our experiments, namely the size by intensity, number, volume, and Z average of the colloidal AuNPs were determined using DLS; however, for simplicity only the size by number have been documented in this study. As many studies have shown previously, when a layer of biomolecules is adsorbed to the nanoparticles, the average particle size is expected to increase, as observed in our experiments through DLS. The polydispersity Index (PDI) was also noted and had an approximate value of 0.2, indicating that our particles have a uniform distribution of AuNPs.

In brief, DLS has shown that the synthesized AuNPs-Cit prepared in water using sodium citrate as both reducing and stabilizing agent at high temperature (~ 95 °C) in presence of sodium hydroxide, were nearly monodisperse with a single size distribution and had an estimate diameter of 25 nm. This was confirmed by the intense single peak observed for DLS, and that correlates to one uniform type of distributed particles in the solution. The small size of our AuNPs, serves to our advantage, since some studies have reported that nanoparticle toxicity is proportional to size and the larger the size the more they portray toxic properties *in-vivo*[145]. Moreover, some studies have also shown that positively charged gold nanoparticles such as cetyltrimethyl ammonium bromide (CTAB- AuNPs), and at their lowest concentration ($0.05\mu\text{M}$), were found to be toxic. This is also an advantage in our favor, since our particles are negatively charged [146].

Initially, the AuNP-Cit showed a negative zeta potential of ~ -45 mV indicating that the citrate molecules were successfully grafted leading to an overall negative charge.

Addition of D2B to AuNPs-citrate colloidal solution caused a red shift (higher wavelength) by about 15 nm in the UV-Vis spectra represented in figure 1, this change in

color might be due to the change in the refractive index around the AuNPs as a result to the attachment of D2B [147]. Furthermore, a successful conjugation of the AuNP-Citrate with D2B was confirmed through the increase in the AuNPs size of almost 38 nm that was revealed by DLS (~25 to ~63 nm size distribution by number). On the other hand, a reduction of 22mV in the overall negative charge of the AuNPs was observed through the Zeta potential measurements (from ~ -45 mV for AuNPs-Cit to -23 mV for AuNP-Cit-D2B). This is not surprising, as the incorporation of an additive such as the proteins will result in a decrease in the overall surface negativity of the AuNPs and therefore the results obtained further highlight a successful conjugation [148].

The UV-visible spectra clearly show a single plasmon absorbance band characteristic of highly stable spherical Au nanoparticle. A schematic figure representation of the resonance phenomena resulting on the surface of the particles is seen in figure 9. Usually, when the incident light interacts with the nanoparticles, there is resonance on the surface of the electrons. This resonance is translated into absorption of the light. This phenomenon is observed due to the fact that the diameter of the nanoparticles is smaller than the wavelength of the light. This causes a polarization of the surface electrons which eventually leads to resonance and is observed at a particular wavelength. The oscillation frequency is governed by four factors: the density of electrons, the electron mass, and the shape and size of the charge distribution. Moreover, the collective oscillation of the electrons is called the plasmon resonance, and in a fairly complex mathematical formula the plasmon frequency can be related to the metal dielectric constant, which is a property that can be measured as a function of wavelength for bulk metal [149].

Therefore, in large, the optical properties of nanoparticles are size and shape dependent, so for example, the surface plasmon absorption band of colloidal nanoparticles is different than that of nanorods [150]. Moreover, when we are adding a protein, such as an antibody in our case, the nanoparticle is being capped and coated, so we are changing the size of the NPs and the plasmon band will shift to a higher wavelength [150]. This notion was observed when the wavelength of maximum absorbance (λ_{max}) was found to be at 525 nm for AuNPs-Citrate and 540 nm for AuNPs-Cit-D2B, indicating that the AuNPs core size are very close to 25 nm as determined by *Image J* analysis of the SEM image of AuNPs-Cit-D2B (image not shown).

Furthermore, as a preliminary indicator of size variation upon conjugation of the antibodies, we observed the color change that was mainly from a red wine to pink-red in color. This color change occurs due to the change in the optical properties of the nanoparticles when then the wavelength and absorption is altered as a consequence of a change in size. Taken together, our results culminate to show that effective conjugation has occurred.

To examine the cytotoxicity of our AuNP-Citrate and AuNP-D2Bs, a WST-1 cell proliferation assay was conducted. WST-1 is slightly red in color and is commonly used to quantitate cell proliferation and viability. The principle behind the assay basically is that WST-1 is a tetrazolium salt that is cleaved to formazan by enzymes in metabolically active cells [151]. Therefore, the amount of formazan dye produced directly correlates to the number of metabolically active cells in the culture. For example, an increase in the number of cells would result in an increase in the formazan and the absorbance of the formed dye is measured colorimetrically on an ELISA reader which is directly

proportional to the number of active cells in the cell culture. In our experiment, PC3-PSMA cells were seeded in 96-well plates and were subjected to different concentrations of AuNPs-Cit and AuNP-Cit-D2B.

The results obtained in our experiment support the non-cytotoxic effects of AuNP-D2B and AuNPs-citrate, since the percent viability remained above 80 % for all the concentrations used and even at the highest concentration of nanoparticles the percent viability was comparable to the control with a 98.4 % and 90 % viability for the AuNPs alone and AuNP-D2B, respectively.

To recapitulate, the nanoparticles did not affect the proliferation of the PC3-PSMA cancer cells, which allow them to be used solely as efficient targeting agents that carry the effective payload or drug to the cancer cells. The results clearly demonstrate the safe nature of our synthesized particles. This is also consistent with the results reported by Vijayakumar *et. al.*, 2012, where the gold nanoparticles coated by citrate did not lead to cytotoxicity to the MCF-7 and PC-3 cells [152]. In fact, the incorporation of surface functionalities such as citrate was mentioned to render the gold nanoparticles as highly biocompatible. The citrate salt initially acts as a reducing agent by forming a layer of citrate ions (negatively charged) over the gold nanoparticles surface, inducing enough electrostatic repulsion between individual particles to keep them well dispersed in the medium. This method provides uniform and fairly spherical nanoparticles [152] along with a negatively charged surface to potentiate the binding of the D2B antibody via the positively charged N terminals and through the attachment of the thiol groups in the cysteine that constitutes the antibody. Overall, the citrate is not only favoring the binding

of the antibodies, but also stabilizing the gold nanoparticles and thereby extending their shelf life [153].

To further investigate on the non cytotoxic nature of our NPs, DNA fragmentation analysis was done by agarose gel electrophoresis in search for cleaved DNA which is a hallmark of apoptosis in cells. The gel shows that the whole genome remained intact and this was observed by the DNA bands that were above the 1kb ladder mark, for all the concentrations used namely 0, 6, 12, and 20 $\mu\text{g/ml}$. Therefore, a plausible conclusion is that our AuNP-D2Bs do not induce apoptosis even at high doses and the results achieved portray the non-cytotoxic nature of the synthesized particles, since no DNA fragments were observed in order to point out apoptotic events. Interestingly, these results are not in line with the results obtained by (Mohan *et.al.*, 2013), in which the DNA fragmentation assay was performed on gold-citrate nanoparticles, but had shown that they induce apoptosis on human lung carcinoma type II epithelial cells (A549 cells). Perhaps, this could be attributed to the fact that they treated the cells for 48 hours instead of 4 hours, although they were only 4.5 nm in size. The authors report that the AuNP-citrate activated caspases intracellularly which induced apoptosis of the cells. Another interesting outcome of their studies revealed that the same conditions did not induce apoptosis in breast cancer cell line MCF-7. The gold nanoparticles functionalized with citrate failed to induce any death response in MCF-7 cell lines [154]. The authors failed to delineate the exact reason for why the NPs did not evoke any apoptotic response in the MCF-7 cell line. In our case, it is evident that unravelling the mechanism of such specific cell responses would definitely enhance the efforts to develop nanoconjugate-based therapeutic strategies per cell type and also to analyze the toxicity of nanomaterial. So

using another cell type such as ovarian cancer cells (SKOV3) for example would help us better understand if cytotoxicity and apoptic events are cellular dependent.

On the other hand, to confirm the binding of the AuNP-D2Bs to the PSMA antigen, flow cytometry was done. Analysis of flow cytometry histograms of three different trials reveal that the FITC fluorescence intensity (FL1) significantly increased as the concentration of AuNP-D2B increased. The goat monoclonal anti-D2B FITC was used as a secondary antibody to D2B, therefore any signal observed is inherently due to the D2B that is successfully complexed with the AuNPs. This implies that AuNP-D2B binding to the surface PSMA increased in a dose dependent manner.

It is worth mentioning that since the cells were treated at 37 °C at the allotted time of 4 hrs then normal cellular mechanisms were taking place and therefore AuNP-D2B bound to the PSMA might have triggered endocytosis and resulting in the internalization of the PSMA receptors which may not have been recognized by the FITC antibody which was only incubated for a period of 1 hour. Lowering the incubation temperature to 4 degrees or using colchicine (microtubule inhibitor), a more intense increase would occur, since endocytosis is impeded or halted, respectively [33, 155]. Such a strategy would result in more PSMA receptors being occupied, resulting in their saturation. Moreover, since we did not permeabilise the cells with a detergent such as triton, we did not allow for the quantification of the internalized receptors and the aim was only to quantitate the surface bound AuNP-D2Bs. Future, flow cytometry experiments, will be done to investigate the internalization of our nanoparticles, in permeabilized cells. On a side note, cells were also treated with AuNPs alone and

detected for FITC fluorescence, to exclude that no non-specific binding is taking place (data not shown).

Although a significant difference was observed between the control and the treated cells, a rough 20 MFI is considered high for a control, so for the benefit of doubt, a normalized graph for the mean FL1 was plotted in order to display the results without the background and noise interference. The modest increment in the signal observed for the control might be due to a fault while adjusting the voltage parameters in the flow cytometer, giving a slightly elevated signal.

Regarding the histogram analysis, incubating PCa cells with 6 $\mu\text{g/mL}$ of AuNP concentration showed a non-significant difference (ns) compared to the control sample. This is in sharp contrast to when, the concentration of AuNP-D2B was increased to 12 $\mu\text{g/mL}$ and 20 $\mu\text{g/mL}$, which resulted in the formation of PSMA-D2B complexes at the cell surface and was evident with the sharp right shift in the graph. However, the difference in the shift at 12 $\mu\text{g/mL}$, is not much depicted by the superimposed histograms as they are evident in the histograms. From a statistical standpoint the results confirm successful binding and imply that the higher the AuNP-D2B concentration the greater the number of bound PSMA receptors in the prostate cancer cells.

Interestingly, only one paper was found to present a similar approach for PSMA targeting, using the same D2B antibody. The study entails the use of carbon nanohorns (CNH) that are conjugated with the antibodies and further complexed with the cisplatin drug [156]. The developed strategy showed fascinating results in terms of PSMA binding, internalization, and drug release. Similarly, flow cytometry was employed to evaluate effective D2B-CN H binding to PSMA receptors. They also reported that

normalization of the mean fluorescence intensity was indispensable due to the variability of the non-specific binding of the secondary antibody FITC-labelled to the cell lines under analysis.

Through this method they were capable to measure the fluorescent signal gain of the samples with respect to the signal of the cells incubated with the secondary antibody FITC labelled alone. Moreover, they assumed that this might be due to limited nonspecific absorption of FITC antibody onto the cell or nanosystem surface [156].

With the objective of highlighting the specificity of our AuNP-D2Bs, a western blot experiment was conducted using the wild type form of the prostate cancer cells (PC3-WT) that are PSMA negative, and compared to the PC3-PSMA cells. Moreover, using the primary antibody alone or complexed to AuNPs, confirmed that the bound antibodies will be recognized by the IgG-HRP secondary antibody, when a separate trial was done and the bands were compared. Actin was used a housekeeping protein since it is constitutively expressed in cells and can be used as a reliable marker for internal control. The actin profile remained consistent with the various treatments showing that normal internal conditions are maintained and that it can be used as a control in the experiment to compare any increase or decrease in band width of the tested proteins with subsequent treatments.

Since no band was observed for the PC3-WT cells, this indicates that the AuNP-D2Bs are PSMA specific. On the other hand, a clear thick band (around 100kDa) of comparable width observed for the D2B and AuNP-D2B treated PC3-PSMA cells in both lanes, not only shows that HRP conjugated IgG antibodies are successfully recognizing the D2B bound on the AuNPs, but also highlights the fact that enough bound antibodies exist on

the nanoparticles to give a comparable signal as to when D2B was used alone. Based on our analysis, we propose additional experiments without primary antibody incubations, while targeting the effect of increasing concentrations of AuNP-D2Bs on PC3-PSMA cells treated at 37 degrees and at 4 degrees to compare the internalization and saturation of receptors, respectively. It is essential to note that the mature form of the PSMA receptor exists in a highly glycosylated profile, which corresponds to its fully functional enzymatic form. Therefore, it is normal to observe a band at the 120 kDa molecular weight mark, which is indicative of the glycosylation of the protein receptor; however, this native conformation of the PSMA is altered upon heating the cell lysate before western blot analysis and hence much of the PSMA exists in its deglycosylated profile [157].

Glycosylation of PSMA is a key factor for the homodimerization that occurs in the Golgi, resulting in its enzymatically active form that is transported via the secretory pathway, to the apical surface of the cell membrane. However, PSMA is at that point still non-covalently associated as a homodimer at the cell surface [158]. A representative sketch can be seen in figure 12. Upon, antibody-induced cross-linking, dimerization occurs and internalization of cell surface PSMA activates different signaling cascades like the MAPK-pathway [159].

Monomer and dimer forms of the receptor usually exist in equilibrium; however, the former is referred to as “immature” as it lacks enzymatic activity [158].

PSMA is described to constitutively undergo internalization from the cell surface and binding of antibodies has shown to increase the rate of PSMA internalization [160]. In LNCaP cells, for example, PSMA undergoes internalization via clathrin-coated pits

followed by accumulation in endosomes [160]. A schematic representation is seen in figure 11.

Taken together, the results obtained in this study indicate for the first time the efficient coating of gold nanoparticles with a PSMA specific antibody termed D2B. Furthermore, their safety was also emphasized and clearly indicated, which highlights the importance AuNPs-D2B exhibit as targeting agents. Future studies shall be aimed at understanding the internalization fate of PSMA induced by AuNP-D2Bs and whether they are degraded in lysosomes or recycled back to the surface. This constitutes an essential prerequisite to decipher the potential applications of therapeutic payloads onto the targeted nanoparticles.

VI. Conclusion

At the dawn of precision medicine, targeted nanovehicles will provide the substantial means to lower cancer associated mortalities specifically with the use of new molecular targets that can be used for multiple disciplines and harnessed through nanotechnology. The milestone of tumor cell-specific multifunctional nanoparticles will enable an increased sensitivity to chemotherapeutics with lower systemic toxicity to patients.

In this study we provide insight on a novel and unequivocal approach to target prostate cancer using gold nanoparticles that are conjugated to an anti-PSMA antibody (D2B). This optimized method proved to be non-cytotoxic, non-apoptotic, and site specific. Therefore, our results highlight the safe and efficient application of our customized particles *in vitro* to transport therapeutic payloads such as siRNA, chemotherapeutic drugs, or DNA. It remains challenging to test whether the single-chain variable fragment (scFv) of D2B outperforms its complete form with respect to its binding affinity and internalization efficiency. A series of further future *in-vitro* and *in-vivo* studies could be done and specifically one that extends on the role played by the nanoparticles *in-vivo* and how these particles interplay with the immune system. It also remains undeniably imperative to perform studies on mice and on PC3 wild type cells, to fully affirm the particles safe nature. This study is part of an ongoing research subjected towards the use of siRNA conjugated to the AuNP-D2Bs to perform gene knockdown.

VII. References

1. John H. Wasson, et al., *A Structured Literature Review of Treatment for Localized Prostate Cancer*. Arch Fam Med. , 2009. **2**: p. 487-493.
2. William C. Olson, W.D.W.H.a.A.K.R., *Clinical Trials of Cancer Therapies Targeting Prostate-Specific Membrane Antigen*. Reviews on Recent Clinical Trials, 2007. **2**: p. 182-190.
3. Daniyal, M., et al., *Epidemiology, Etiology, Diagnosis and Treatment of Prostate Cancer*. Asian Pacific Journal of Cancer Prevention, 2014. **15**(22): p. 9575-9578.
4. Jared Cox and C.L. Amling, *Current decision-making in prostate cancer therapy*. Current Opinion in Urology 2008. **18**: p. 275-278.
5. Masanori Noguchi, et al., *Immunotherapy in prostate cancer: challenges and opportunities*. Immunotherapy, 2016.
6. Joshi J. Alumkal and T.M. Beer, *Raising the Bar for Therapeutic Trials in Advanced Prostate Cancer*. Journal of Clinical Oncology, 2016. **34**(25): p. 2958-2960.
7. Eton, D.T. and S.J. Lepore, *Prostate cancer and health-related quality of life: a review of the literature*. Psychooncology, 2002. **11**(4): p. 307-26.
8. Flores, O., et al., *PSMA-Targeted Theranostic Nanocarrier for Prostate Cancer*. Theranostics, 2017. **7**(9): p. 2477-2494.
9. Goncalves, A.S., A.S. Macedo, and E.B. Souto, *Therapeutic nanosystems for oncology nanomedicine*. Clin Transl Oncol 2012 **14**: p. 883-890.
10. Hans Lilja, et al., *Seminal Vesicle-secreted Proteins and Their Reactions during Gelation and Liquefaction of Human Semen*. J. Chin. Invest., 1987: p. 281-285.
11. Balk, S.P., Y.J. Ko, and G.J. Bubley, *Biology of prostate-specific antigen*. J Clin Oncol, 2003. **21**(2): p. 383-91.
12. Carter, H.B., *Prostate cancers in men with low PSA levels--must we find them?* N Engl J Med, 2004. **350**(22): p. 2292-4.
13. Gerald P. Murphy, et al., *Evaluation and Comparison of Two New Prostate Carcinoma Markers*. Cancer, 1996. **78**(4): p. 809-818.
14. SHUSEI IKEGAMI, et al., *Targeting Gene Therapy for Prostate Cancer Cells by Liposomes Complexed with Anti-Prostate-Specific Membrane Antigen Monoclonal Antibody*. Human Gene Therapy, 2006. **17**: p. 997-1005.
15. Al-Yasiri, A.Y., et al., *Mangiferin functionalized radioactive gold nanoparticles (MGF-(198)AuNPs) in prostate tumor therapy: green nanotechnology for production, in vivo tumor retention and evaluation of therapeutic efficacy*. Dalton Trans, 2017. **46**(42): p. 14561-14571.
16. Pedrosa, A.R., et al., *Notch signaling dynamics in the adult healthy prostate and in prostatic tumor development*. Prostate, 2016. **76**(1): p. 80-96.
17. Marika J. Linja, et al., *Amplification and Overexpression of Androgen Receptor Gene in Hormone-Refractory Prostate Cancer*. American Association for Cancer Research, 2001. **61**: p. 3550-3555.
18. Rajasekaran, A.K., G. Anilkumar, and J.J. Christiansen, *Is prostate-specific membrane antigen a multifunctional protein?* Am J Physiol Cell Physiol, 2005. **288**(5): p. C975-81.
19. Milowsky, M.I., et al., *Vascular targeted therapy with anti-prostate-specific membrane antigen monoclonal antibody J591 in advanced solid tumors*. J Clin Oncol, 2007. **25**(5): p. 540-7.
20. Banerjee, R., et al., *Anisamide-targeted stealth liposomes: a potent carrier for targeting doxorubicin to human prostate cancer cells*. Int J Cancer, 2004. **112**(4): p. 693-700.
21. Virgolini, I., et al., *Current status of theranostics in prostate cancer*. Eur J Nucl Med Mol Imaging, 2017.
22. Nguyen, D.P., et al., *Induction of PSMA and Internalization of an Anti-PSMA mAb in the Vascular Compartment*. Mol Cancer Res, 2016. **14**(11): p. 1045-1053.

23. Langut, Y., et al., *PSMA-targeted polyinosine/polycytosine vector induces prostate tumor regression and invokes an antitumor immune response in mice*. Proc Natl Acad Sci U S A, 2017. **114**(52): p. 13655-13660.
24. Jain, S., D.G. Hirst, and J.M. O'Sullivan, *Gold nanoparticles as novel agents for cancer therapy*. Br J Radiol, 2012. **85**(1010): p. 101-13.
25. Mazzocco, C., et al., *In vivo imaging of prostate cancer using an anti-PSMA scFv fragment as a probe*. Sci Rep, 2016. **6**: p. 23314.
26. Sam S. Chang, M., *Overview of Prostate-Specific Membrane Antigen*. REVIEWS IN UROLOGY, 2004. **6**
27. Lutje, S., et al., *Targeting human prostate cancer with 111In-labeled D2B IgG, F(ab')₂ and Fab fragments in nude mice with PSMA-expressing xenografts*. Contrast Media Mol Imaging, 2015. **10**(1): p. 28-36.
28. Lutje, S., et al., *Dual-Modality Image-Guided Surgery of Prostate Cancer with a Radiolabeled Fluorescent Anti-PSMA Monoclonal Antibody*. J Nucl Med, 2014. **55**(6): p. 995-1001.
29. Frigerio, B., et al., *Effect of radiochemical modification on biodistribution of scFvD2B antibody fragment recognising prostate specific membrane antigen*. Immunology Letters, 2015. **168**(1): p. 105-110.
30. Tagawa, S.T., et al., *Anti-prostate-specific membrane antigen-based radioimmunotherapy for prostate cancer*. Cancer, 2010. **116**(4 Suppl): p. 1075-83.
31. Sam S. Chang, et al., *Comparison of Anti-Prostate Specific Membrane Antigen Antibodies and other Immunomarkers In Metastatic Prostate Carcinoma*. Urology, 2001. **57**(6): p. 1179-1183.
32. Frigerio, B., et al., *A single-chain fragment against prostate specific membrane antigen as a tool to build theranostic reagents for prostate cancer*. Eur J Cancer, 2013. **49**(9): p. 2223-32.
33. Jie Lu, et al., *Mesoporous Silica Nanoparticles for Cancer Therapy: Energy-Dependent Cellular Uptake and Delivery of Paclitaxel to Cancer Cells*. Nanobiotechnol 2007. **3**: p. 89-95.
34. He Liu, et al., *Constitutive and Antibody-induced Internalization of Prostate-specific Membrane Antigen*. CANCER RESEARCH, 1998. **58**: p. 4055-4060.
35. Khlebtsov, N. and L. Dykman, *Biodistribution and toxicity of engineered gold nanoparticles: a review of in vitro and in vivo studies*. Chem Soc Rev, 2011. **40**(3): p. 1647-71.
36. Chang, S.S., *Overview of Prostate-Specific Membrane Antigen*. REVIEWS IN UROLOGY, 2004. **6**(10).
37. V. L. Kumar, P.K.M., *Prostate Gland: Structure, Functions and Regulation*. International Urology and Nephrology 1995. **27**(3): p. 231-243
38. Chen, S.L., et al., *Prostate Cancer Mortality-To-Incidence Ratios Are Associated with Cancer Care Disparities in 35 Countries*. Sci Rep, 2017. **7**: p. 40003.
39. Keith R.Loeb and L. A.Loeb, *Significance of multiple mutations in cancer*. Carcinogenesis, 2000. **21**(3): p. 379-385.
40. Bubendorf, L., et al., *Metastatic patterns of prostate cancer: An autopsy study of 1,589 patients*. Human Pathology, 2000. **31**(5): p. 578-583.
41. Forbes, L.J., et al., *Risk factors for delay in symptomatic presentation: a survey of cancer patients*. Br J Cancer, 2014. **111**(3): p. 581-8.
42. DeSantis, C.E., et al., *Cancer treatment and survivorship statistics, 2014*. CA Cancer J Clin, 2014. **64**(4): p. 252-71.
43. Torre, L.A., et al., *Global cancer statistics, 2012*. CA Cancer J Clin, 2015. **65**(2): p. 87-108.
44. Ferlay, J., et al., *Cancer incidence and mortality worldwide: sources, methods and major patterns in GLOBOCAN 2012*. Int J Cancer, 2015. **136**(5): p. E359-86.
45. Global Burden of Disease Cancer, C., et al., *The Global Burden of Cancer 2013*. JAMA Oncol, 2015. **1**(4): p. 505-27.

46. Hayes, J.H. and M.J. Barry, *Screening for prostate cancer with the prostate-specific antigen test: a review of current evidence*. JAMA, 2014. **311**(11): p. 1143-9.
47. Elgqvist, J., *Nanoparticles as Theranostic Vehicles in Experimental and Clinical Applications-Focus on Prostate and Breast Cancer*. Int J Mol Sci, 2017. **18**(5).
48. Pan, M.H., et al., *Biodistributions of 177Lu- and 111In-labeled 7E11 antibodies to prostate-specific membrane antigen in xenograft model of prostate cancer and potential use of 111In-7E11 as a pre-therapeutic agent for 177Lu-7E11 radioimmunotherapy*. Mol Imaging Biol, 2009. **11**(3): p. 159-66.
49. van Rij, C.M., et al., *Pretargeted Radioimmunotherapy of Prostate Cancer with an Anti-TROP-2xAnti-HSG Bispecific Antibody and a (177)Lu-Labeled Peptide*. Cancer Biother Radiopharm, 2014. **29**(8): p. 323-9.
50. Mottet N., et al., *Guidelines on Prostate Cancer*. European Association of Urology, 2015: p. 1–137.
51. Bostwick, D.G., et al., *Human prostate cancer risk factors*. Cancer, 2004. **101**(10 Suppl): p. 2371-490.
52. Andrew M. D. Wolf, et al., *American Cancer Society Guideline for the Early Detection of Prostate Cancer*. CA: A Cancer Journal for Clinicians, 2010. **60**: p. 70-98.
53. Henrik Gronberg, Lena Damber, and Jan Erik Damber, *Familial Prostate Cancer in Sweden: A Nationwide Register Cohort Study*. American Cancer Society **77**: p. 138-143.
54. CRAWFORD, E.D., *EPIDEMIOLOGY OF PROSTATE CANCER*. Urology, 2003. **62**: p. 3-12.
55. Kolonel, L.N., D. Altshuler, and B.E. Henderson, *The multiethnic cohort study: exploring genes, lifestyle and cancer risk*. Nat Rev Cancer, 2004. **4**(7): p. 519-27.
56. Frigerio, B., et al., *Full preclinical validation of the 123 I-labeled anti-PSMA antibody fragment ScFvD2B for prostate cancer imaging*. Oncotarget, 2017. **8**(7): p. 10919-10930.
57. Machulkin, A.E., et al., *Nanohybride Materials Based on Magnetite-Gold Nanoparticles for Diagnostics of Prostate Cancer: Synthesis and In Vitro Testing*. Bulletin of Experimental Biology and Medicine, 2016. **161**(5): p. 706-710.
58. SMITH, D.S. and W.J. CATALONA, *INTEREXAMINER VARIABILITY OF DIGITAL RECTAL EXAMINATION IN DETECTING PROSTATE CANCER*. Urology, 1995. **45**(1).
59. IM, T., Pauler DK, and G.P.e. al., *Prevalence of prostate cancer among men with a prostate-specific antigen level < or =4.0 ng per milliliter*. New England Journal of Medicine, 2004. **350**(22): p. 2239-2246.
60. BRAUN, K., et al., *High-resolution flow cytometry: a suitable tool for monitoring aneuploid prostate cancer cells after TMZ and TMZ-BioShuttle treatment*. Int J Med Sci, 2009. **6**: p. 338-347.
61. Peyromaure, M., et al., *[Characteristics of prostate cancer in men less than 50-year-old]*. Prog Urol, 2009. **19**(11): p. 803-9.
62. Ibrahim, T., et al., *Pathogenesis of osteoblastic bone metastases from prostate cancer*. Cancer, 2010. **116**(6): p. 1406-18.
63. Sun, H., et al., *Oligonucleotide aptamers: new tools for targeted cancer therapy*. Mol Ther Nucleic Acids, 2014. **3**: p. e182.
64. Sanna, V. and M. Sechi, *Nanoparticle therapeutics for prostate cancer treatment*. Nanomedicine, 2012. **8 Suppl 1**: p. S31-6.
65. Anil K. Patri, et al., *Synthesis and in Vitro Testing of J591 Antibody-Dendrimer Conjugates for Targeted Prostate Cancer Therapy*. Bioconjugate Chem, 2004. **15**: p. 1174-1181.
66. Kaittanis, C., et al., *Targetable Clinical Nanoparticles for Precision Cancer Therapy Based on Disease-Specific Molecular Inflection Points*. Nano Lett, 2017. **17**(11): p. 7160-7168.

67. Sajib Chakraborty and T. Rahman, *The difficulties in cancer treatment*. *ecancermedicalsecience*, 2012. **6**(16).
68. Chang, S.S., Gaudin, P. B., Reuter, V. E., and Heston, W. and D. W., *Prostate-specific membrane antigen: Present and future application*. *Urology* 2000. **55**: p. 622-629.
69. Ron S. Israeli, C.T.P., John G. Corr, William R. Fair, and Warren D. W. Heston, *Expression of the Prostate-specific Membrane Antigen*. *Cancer Research* 1994. **54**: p. 1807-1811.
70. Hofman, M.S., et al., *Prostate-specific Membrane Antigen PET: Clinical Utility in Prostate Cancer, Normal Patterns, Pearls, and Pitfalls*. *Radiographics*, 2018. **38**(1): p. 200-217.
71. Davis, M.I., et al., *Crystal structure of prostate-specific membrane antigen, a tumor marker and peptidase*. *Proc Natl Acad Sci U S A*, 2005. **102**(17): p. 5981-6.
72. Backhaus, P., et al., *Targeting PSMA by radioligands in non-prostate disease-current status and future perspectives*. *Eur J Nucl Med Mol Imaging*, 2018.
73. Guillemard, V., and Saragovi, H. U. , *Taxane-Antibody Conjugates Afford Potent Cytotoxicity, Enhanced Solubility, and Tumor Target Selectivity*. *Cancer Res.*, 2001. **61**: p. 694-699.
74. Manuel Arruebo, Mónica Valladares, and a.A. Gonz´alez-Fern´andez, *Antibody-Conjugated Nanoparticles for Biomedical Applications*. *Journal of Nanomaterials* 2009 **2009**: p. 24.
75. Fl´avia Sousa, et al., *Nanoparticles for the delivery of therapeutic antibodies: Dogma or promising strategy?* *Expert Opinion on Drug Delivery*, 2016.
76. Pietersz, G.A., et al., *Therapeutic targeting in nanomedicine: the future lies in recombinant antibodies*. *Nanomedicine (Lond.)*, 2017: p. 1873-1889.
77. Buzea, C., I.I. Pacheco, and K. Robbie, *Nanomaterials and nanoparticles: Sources and toxicity*. *Biointerphases*, 2007. **2**(4): p. MR17-MR71.
78. Ahmed, N., H. Fessi, and A. Elaissari, *Theranostic applications of nanoparticles in cancer*. *Drug Discov Today*, 2012. **17**(17-18): p. 928-34.
79. Rizzo, L.Y., et al., *Recent progress in nanomedicine: therapeutic, diagnostic and theranostic applications*. *Curr Opin Biotechnol*, 2013. **24**(6): p. 1159-66.
80. Chowdhury, P., et al., *Magnetic nanoformulations for prostate cancer*. *Drug Discov Today*, 2017. **22**(8): p. 1233-1241.
81. Tse, B.W.-C., et al., *PSMA-targeting iron oxide magnetic nanoparticles enhance MRI of preclinical prostate cancer*. *Nanomedicine (Lond)*, 2015. **10**(3): p. 375-386.
82. Katharina A Sterenczak, et al., *Longitudinal MRI contrast enhanced monitoring of early tumour development with manganese chloride (MnCl₂) and superparamagnetic iron oxide nanoparticles (SPIOs) in a CT1258 based in vivo model of prostate cancer*. *BioMed Central Cancer* 2012. **12**(284): p. 1-11.
83. Agemy, L., et al., *Nanoparticle-induced vascular blockade in human prostate cancer*. *Blood*, 2010. **116**(15): p. 2847-56.
84. Cui, D., et al., *Gastrin-releasing peptide receptor-targeted gadolinium oxide-based multifunctional nanoparticles for dual magnetic resonance/fluorescent molecular imaging of prostate cancer*. *International Journal of Nanomedicine*, 2017. **Volume 12**: p. 6787-6797.
85. Hu, F., et al., *High-performance nanostructured MR contrast probes*. *Nanoscale*, 2010. **2**(10): p. 1884-91.
86. Lentschig M.G., et al., *Breath-hold gadolinium-enhanced MR angiography of the major vessels at 1.0 t: Dose-response findings and angiographic correlation*. *Radiology*, 1998. **208**: p. 353-357.
87. K. Ni, et al., *Geometrical confined ultrasmall gadolinium oxide nanoparticles boost the T1 contrast ability*. *Nanoscale* 2016. **14**.

88. Gao, X., et al., *Mn-doped ZnSe d-dots-based alpha-methylacyl-CoA racemase probe for human prostate cancer cell imaging*. *Anal Bioanal Chem*, 2012. **402**(5): p. 1871-7.
89. Mijnenonckx, K., et al., *Antimicrobial silver: uses, toxicity and potential for resistance*. *Biometals*, 2013. **26**(4): p. 609-21.
90. Yamada, M., M. Foote, and T.W. Prow, *Therapeutic gold, silver, and platinum nanoparticles*. *Wiley Interdiscip Rev Nanomed Nanobiotechnol*, 2015. **7**(3): p. 428-45.
91. Vlăscianu, G.M., et al., *Silver nanoparticles in cancer therapy*. 2016: p. 29-56.
92. Firdhouse, M.J. and P. Lalitha, *Biosynthesis of silver nanoparticles using the extract of *Alternanthera sessilis*-antiproliferative effect against prostate cancer cells*. *Cancer Nanotechnol*, 2013. **4**(6): p. 137-143.
93. Mohammadzadeh, R., *Hypothesis: silver nanoparticles as an adjuvant for cancertherapy*. *Adv Pharm Bull*, 2012. **2**(1): p. 133.
94. Wang, H., et al., *Label-free electrochemical immunosensor for prostate-specific antigen based on silver hybridized mesoporous silica nanoparticles*. *Anal Biochem*, 2013. **434**(1): p. 123-7.
95. He, Y., et al., *Synthesis, characterization and evaluation cytotoxic activity of silver nanoparticles synthesized by Chinese herbal *Cornus officinalis* via environment friendly approach*. *Environ Toxicol Pharmacol*, 2017. **56**: p. 56-60.
96. al., K.e., *Neuropilin-1-Targeted Gold Nanoparticles Enhance Therapeutic Efficacy of Platinum(IV) Drug for Prostate Cancer Treatment*. *ACS Nano*, 2014. **8**(5): p. 4205-4220.
97. Li, M., et al., *A novel signal amplification system fabricated immunosensor based on Au nanoparticles and mesoporous trimetallic PdPtCu nanospheres for sensitive detection of prostate specific antigen*. *Sensors and Actuators B: Chemical*, 2018. **261**: p. 22-30.
98. Zhang, B., et al., *Redox and catalysis 'all-in-one' infinite coordination polymer for electrochemical immunosensor of tumor markers*. *Biosens Bioelectron*, 2015. **64**: p. 6-12.
99. Spain, E., et al., *Detection of prostate specific antigen based on electrocatalytic platinum nanoparticles conjugated to a recombinant scFv antibody*. *Biosens Bioelectron*, 2016. **77**: p. 759-66.
100. Taylor, R.M. and L.O. Sillerud, *Paclitaxel-loaded iron platinum stealth immunomicelles are potent MRI imaging agents that prevent prostate cancer growth in a PSMA-dependent manner*. *Int J Nanomedicine*, 2012. **7**: p. 4341-52.
101. Singh, B.R., et al., *ROS-mediated apoptotic cell death in prostate cancer LNCaP cells induced by biosurfactant stabilized CdS quantum dots*. *Biomaterials*, 2012. **33**(23): p. 5753-67.
102. He, X. and N. Ma, *An overview of recent advances in quantum dots for biomedical applications*. *Colloids Surf B Biointerfaces*, 2014. **124**: p. 118-31.
103. IGOR L. MEDINTZ, et al., *Quantum dot bioconjugates for imaging, labelling and sensing*. *nature materials*, 2005. **4**: p. 435-446.
104. Hooisweng Ow, et al., *Bright and Stable Core-Shell Fluorescent Silica Nanoparticles*. *Nano Letters*, 2005. **5**(1): p. 113-117.
105. Andrew A. Burns, et al., *Fluorescent Silica Nanoparticles with Efficient Urinary Excretion for Nanomedicine*. *Nano Lett*, 2009. **9**(1): p. 442-448.
106. Lin, Z., et al., *A novel aptamer functionalized CuInS₂ quantum dots probe for daunorubicin sensing and near infrared imaging of prostate cancer cells*. *Anal Chim Acta*, 2014. **818**: p. 54-60.
107. Garcia-Cortes, M., et al., *Sensitive prostate specific antigen quantification using dihydrolipoic acid surface-functionalized phosphorescent quantum dots*. *Anal Chim Acta*, 2017. **987**: p. 118-126.
108. Zhao, Y., et al., *Near-Infrared Quantum Dot and (89)Zr Dual-Labeled Nanoparticles for in Vivo Cerenkov Imaging*. *Bioconjug Chem*, 2017. **28**(2): p. 600-608.

109. Malekzad, H., et al., *Highly sensitive immunosensing of prostate specific antigen using poly cysteine capped by graphene quantum dots and gold nanoparticle: A novel signal amplification strategy*. *Int J Biol Macromol*, 2017. **105**(Pt 1): p. 522-532.
110. Kroon, J., et al., *Liposomal nanomedicines in the treatment of prostate cancer*. *Cancer Treat Rev*, 2014. **40**(4): p. 578-84.
111. Abolfazl Akbarzadeh, et al., *Liposome: classification, preparation, and applications*. *Nanoscale Research Letters* 2013. **8**(102): p. 1-9.
112. Maeda, H., et al., *Tumor Vascular Permeability and the EPR Effect in Macromolecular Therapeutics: A Review*. *J. Controlled Release*, 2000. **65**(1-2): p. 271-284.
113. Prabhakar, U., et al., *Challenges and key considerations of the enhanced permeability and retention effect for nanomedicine drug delivery in oncology*. *Cancer Res*, 2013. **73**(8): p. 2412-7.
114. Al-Azayzih, A., et al., *Liposome-mediated delivery of the p21 activated kinase-1 (PAK-1) inhibitor IPA-3 limits prostate tumor growth in vivo*. *Nanomedicine: Nanotechnology, Biology and Medicine*, 2016. **12**(5): p. 1231-1239.
115. Pugazhendhi, A., et al., *Inorganic nanoparticles: A potential cancer therapy for human welfare*. *Int J Pharm*, 2018. **539**(1-2): p. 104-111.
116. RAJESH L. THANGAPAZHAM, et al., *Evaluation of a nanotechnology-based carrier for delivery of curcumin in prostate cancer cells*. *INTERNATIONAL JOURNAL OF ONCOLOGY*, 2008. **32**: p. 1119-1123.
117. Yeh, C.Y., et al., *Peptide-conjugated nanoparticles for targeted imaging and therapy of prostate cancer*. *Biomaterials*, 2016. **99**: p. 1-15.
118. Sauvage, F., et al., *Formulation and in vitro efficacy of liposomes containing the Hsp90 inhibitor 6BrCaQ in prostate cancer cells*. *Int J Pharm*, 2016. **499**(1-2): p. 101-109.
119. Xiang, B., et al., *PSA-responsive and PSMA-mediated multifunctional liposomes for targeted therapy of prostate cancer*. *Biomaterials*, 2013. **34**(28): p. 6976-91.
120. Carabineiro, S.A.C., *Applications of Gold Nanoparticles in Nanomedicine: Recent Advances in Vaccines*. *Molecules*, 2017. **22**(5).
121. Ravi Shuklaa, et al., *Laminin receptor specific therapeutic gold nanoparticles (198AuNP-EGCG) show efficacy in treating prostate cancer*. *PNAS*, 2012. **109**(31): p. 12426-12431.
122. Guo, J., et al., *Bioconjugated gold nanoparticles enhance cellular uptake: A proof of concept study for siRNA delivery in prostate cancer cells*. *Int J Pharm*, 2016. **509**(1-2): p. 16-27.
123. Oh, M.H., et al., *Genetically Programmed Clusters of Gold Nanoparticles for Cancer Cell-Targeted Photothermal Therapy*. *ACS Appl Mater Interfaces*, 2015. **7**(40): p. 22578-86.
124. Lu, L., et al., *Gold-chrysophanol nanoparticles suppress human prostate cancer progression through inactivating AKT expression and inducing apoptosis and ROS generation in vitro and in vivo*. *International Journal of Oncology*, 2017. **51**(4): p. 1089-1103.
125. Li-Chu Tsai, et al., *EGCG/gelatin-doxorubicin gold nanoparticles enhance therapeutic efficacy of doxorubicin for prostate cancer treatment*. *Nanomedicine (Lond)*, 2016. **11** (1): p. 9-30.
126. Rodriguez, C., et al., *Gold nanoparticle triggered dual optoplasmonic-impedimetric sensing of prostate-specific antigen on interdigitated porous silicon platforms*. *Sensors and Actuators B: Chemical*, 2018.
127. Ana I. Barbosa, et al., *Towards One-Step Quantitation of Prostate-Specific Antigen (PSA) in Microfluidic Devices: Feasibility of Optical Detection with Nanoparticle Labels*. *BioNanoSci.*, 2017. **7**: p. 718–726.
128. M. Pal, R.K., *Detection of prostate cancer risk factor immunosensor based deposition of graphene layer decorated gold nanoparticles*. *Analytical Biochemistry* 2017.

129. Suresh, L., et al., *Development of an electrochemical immunosensor based on gold nanoparticles incorporated chitosan biopolymer nanocomposite film for the detection of prostate cancer using PSA as biomarker*. *Enzyme Microb Technol*, 2018. **112**: p. 43-51.
130. Vural, T., et al., *Electrochemical immunoassay for detection of prostate specific antigen based on peptide nanotube-gold nanoparticle-polyaniline immobilized pencil graphite electrode*. *J Colloid Interface Sci*, 2018. **510**: p. 318-326.
131. Karl Butterworth, J.N., Mihaela Ghita, Soraia Rosa, Pankaj Chaudhary, et al., *Preclinical evaluation of gold-DTDTA nanoparticles as theranostic agents in prostate cancer radiotherapy*. *Nanomedicine*, 2016. **11**(16): p. 2035-2047.
132. Stefan Harmsen, M.A.W., Ruimin Huang, Moritz F Kircher, *Cancer imaging using surface-enhanced resonance Raman scattering nanoparticles*. *Nature Protocols* 2017. **12**(7): p. 1400-1414.
133. Sattarahmady, N., A. Rahi, and H. Heli, *A signal-on built in-marker electrochemical aptasensor for human prostate-specific antigen based on a hairbrush-like gold nanostructure*. *Sci Rep*, 2017. **7**(1): p. 11238.
134. Srivastava, M., et al., *A comparative Study of Aptasensor Vs Immunosensor for Label-Free PSA Cancer Detection on GQDs-AuNRs Modified Screen-Printed Electrodes*. *Sci Rep*, 2018. **8**(1): p. 1923.
135. Huang, L., et al., *Prostate-specific antigen immunosensing based on mixed self-assembled monolayers, camel antibodies and colloidal gold enhanced sandwich assays*. *Biosens Bioelectron*, 2005. **21**(3): p. 483-90.
136. Kristine M. Mayle, K.R.D., Vincent K. Wong, Kevin Y. Chen,, et al., *Engineering A11 Minibody-Conjugated, Polypeptide-Based Gold Nanoshells for Prostate Stem Cell Antigen (PSCA)-Targeted Photothermal Therapy*. *Journal of Laboratory Automation*, 2016: p. 1-10.
137. Kim, W., et al., *Selective uptake of epidermal growth factor-conjugated gold nanoparticle (EGF-GNP) facilitates non-thermal plasma (NTP)-mediated cell death*. *Sci Rep*, 2017. **7**(1): p. 10971.
138. Lechtman, E. and J.P. Pignol, *Interplay between the gold nanoparticle sub-cellular localization, size, and the photon energy for radiosensitization*. *Sci Rep*, 2017. **7**(1): p. 13268.
139. Allison M. Khoo, et al., *Radiosensitization of Prostate Cancers In Vitro and In Vivo to Erbium-filtered Orthovoltage X-rays Using Actively Targeted Gold Nanoparticles*. *Scientific Reports*, 2017. **7**(18044): p. 1-13.
140. Kasten, B.B., et al., *Targeting prostate cancer cells with PSMA inhibitor-guided gold nanoparticles*. *Bioorg Med Chem Lett*, 2013. **23**(2): p. 565-8.
141. Giljohann, D.A., et al., *Gold nanoparticles for biology and medicine*. *Angew Chem Int Ed Engl*, 2010. **49**(19): p. 3280-94.
142. Nghiem, T.H.L., et al., *Synthesis, capping and binding of colloidal gold nanoparticles to proteins*. *Advances in Natural Sciences: Nanoscience and Nanotechnology*, 2010. **1**(2): p. 025009.
143. Scott, C.J., et al., *Immunocolloidal targeting of the endocytotic siglec-7 receptor using peripheral attachment of siglec-7 antibodies to poly(lactide-co-glycolide) nanoparticles*. *Pharm Res*, 2008. **25**(1): p. 135-46.
144. Jazayeri, M.H., et al., *Various methods of gold nanoparticles (GNPs) conjugation to antibodies*. *Sensing and Bio-Sensing Research*, 2016. **9**: p. 17-22.
145. Mironava, T., et al., *Gold nanoparticles cellular toxicity and recovery: effect of size, concentration and exposure time*. *Nanotoxicology*, 2010. **4**(1): p. 120-37.
146. Connor, E.E., et al., *Gold nanoparticles are taken up by human cells but do not cause acute cytotoxicity*. *Small*, 2005. **1**(3): p. 325-7.

147. Esmaeil Shahriari, W.Mahmood Mat Yunus, and E. Saion, *Effect of particle size on nonlinear refractive index of Au nanoparticle in PVA solution*. Brazilian Journal of Physics, 2010. **40**(2): p. 256-260.
148. Honary, S. and F. Zahir, *Effect of Zeta Potential on the Properties of Nano-Drug Delivery Systems - A Review (Part 1)*. Tropical Journal of Pharmaceutical Research, 2013. **12**(2).
149. K. Lance Kelly, et al., *The Optical Properties of Metal Nanoparticles: The Influence of Size, Shape, and Dielectric Environment*. J. Phys. Chem, 2003. **107**: p. 668-677.
150. Amendola, V., et al., *Surface plasmon resonance in gold nanoparticles: a review*. J Phys Condens Matter, 2017. **29**(20): p. 203002.
151. Guertler, A., et al., *The WST survival assay: an easy and reliable method to screen radiation-sensitive individuals*. Radiat Prot Dosimetry, 2011. **143**(2-4): p. 487-90.
152. Vijayakumar, S. and S. Ganesan, *In Vitro Cytotoxicity Assay on Gold Nanoparticles with Different Stabilizing Agents*. Journal of Nanomaterials, 2012. **2012**: p. 1-9.
153. Zhang, S., Y. Moustafa, and Q. Huo, *Different interaction modes of biomolecules with citrate-capped gold nanoparticles*. ACS Appl Mater Interfaces, 2014. **6**(23): p. 21184-92.
154. Mohan, J.C., et al., *Functionalised gold nanoparticles for selective induction of in vitro apoptosis among human cancer cell lines*. Journal of Experimental Nanoscience, 2013. **8**(1): p. 32-45.
155. Jun-Sung Kim, et al., *Cellular uptake of magnetic nanoparticle is mediated through energy-dependent endocytosis in A549 cells*. J. Vet. Sci, 2006. **7**(4): p. 321-326.
156. M. I. Lucio, et al., *Targeted killing of prostate cancer cells using antibody-drug conjugated carbon nanohorns* Journal of Materials Chemistry B, 2017: p. 13.
157. K. J. Henle, et al., *Prompt protein glycosylation during acute heat stress*. Experimental Cell Research 1993. **207**: p. 245-251.
158. Schulke, N., et al., *The homodimer of prostate-specific membrane antigen is a functional target for cancer therapy*. Proc Natl Acad Sci U S A, 2003. **100**(22): p. 12590-5.
159. Hotchin, N., et al., *The Prostate Specific Membrane Antigen Regulates the Expression of IL-6 and CCL5 in Prostate Tumour Cells by Activating the MAPK Pathways*. PLoS ONE, 2009. **4**(2): p. e4608.
160. He Liu, et al., *Constitutive and Antibody-induced Internalization of Prostate-specific Membrane Antigen*. CANCER RESEARCH 1998. **58**(4055-4060).
161. (<https://patents.google.com/patent/WO2009130575A2/en>)

VIII. Tables and Figures

Table 1: Summary of the gold nanoparticles employed for the targeted therapy or diagnosis of prostate cancer. The table summarizes the novel strategies employed for prostate cancer theranostics using gold nanoparticles in a chronological order (2005-2018).

Type of AuNPs	Application	Target	Result	Reference
anti-PSA camel antibody coated to streptavidin coated AuNPs	A PSA sandwich modified biosensor was used and quantification was done using a surface plasmon resonance instrument.	Not applicable	Major enhancement in sensitivity of PSA detection was observed with a limit of detection as low as 1 ng/mL.	Huang <i>et al.</i> , (2005), [135]
(EGCG) tagged ¹⁹⁸ AuNPs	PC3-xenograft SCID mice /Intratumorally	Laminin receptors	80% reduction of tumor volumes after 28 days	Shukla <i>et al.</i> , (2012), [121]
AuNP- biotin-PEG12-CTT54 inhibitor	Prostate cancer cells were targeted with PSMA inhibitor (CTT54)-guided gold NPs.	PSMA receptor	Higher and selective binding to LNCaP cells compared to control non-targeted AuNPs in a time-dependent manner.	Kasten <i>et al.</i> , (2013), [108]
Phage-AuNP	PC3-cells	PSMA receptors	Target specific photothermal therapy	Oh <i>et al.</i> , (2015), [123]
AuNPs-PEG-Tf/ AuNPs-PEI-FA.siRNA	LNCap cells /PC3-cells	Transferrin and Folate receptors	-Cellular uptake and non-cytotoxicity of the AuNPs-PEG-Tf was observed. -RelA gene silencing after 24hrs was observed for AuNPs-PEI-FA.siRNA.	Guo <i>et al.</i> , (2016), [122]
EGCG-AuNPs.DOX	PC3-cells	Laminin Receptors	Enhanced receptor mediated endocytosis and induction of apoptosis after 24hrs	Tsai <i>et al.</i> , (2016), [125]
Au@DTDTPA	CT-contrast imaging and radiotherapy in PC3, DU 145, PNT2-C2 cells, and Human PC3 xenograft tumor models.	Not applicable	10 % CT imaging enhancement, increased cytotoxicity after 24hr exposure to the NPs, and tumor growth delay of 17 days.	Butterworth <i>et al.</i> , (2016), [131]
A11 minibody-conjugated to a gold nanoshell	Photothermal therapy on PSCA-transfected 22Rv1 prostate cancer cells	PSCA receptor	Enhanced localized killing of prostate cancer cells compared to nontargeted gold nanoshells.	Mayle <i>et al.</i> , (2016), [136]
GF- ¹⁹⁸ AuNP	CF-1 mice/intratumorally	Laminin receptors	80% retention of the injected dose (ID) in prostate tumors after 24 h. By three weeks post treatment, over 5 fold reduction of the tumor volumes.	Al Yasiri <i>et al.</i> , (2017), [15]
Chrysophanol-AuNPs	LNCap/PC3/DU 145	Not Applicable	Inactivating AKT expression and inducing apoptosis and ROS generation.	Lu <i>et al.</i> (2017), [124]
Silver	microfluidic immunoassay	Not applicable	PSA limit of detection range from 10 to 100 ng/mL.	Barbosa <i>et al.</i> , (2017), [127]

enhanced AuNPs	precoated with CapAb and layered with immobilized gold NPs.			
Au-GrO	Au-GrO on platinum electrode, immobilized with anti PSA	Not applicable	immunosensor had a PSA limit of detection of 0.24 fg/mL.	Pal <i>et al.</i> , (2017), [128]
AuNPs encapsulated with a silica shell	Injected intratumorally in Hi-Myc mouse	Not applicable	Highly sensitive tumor detection with contrast-enhanced Raman imaging.	Harmsen <i>et al.</i> , (2017), [132]
Hairbrush-like gold nanostructure	NPs as transducers to fabricate a signal-on built in-marker electrochemical aptasensor for the detection of PSA	Not applicable	The aptasensor detected PSA with a limit of detection of 50 pg mL ⁻¹ .	Sattarahmady <i>et al.</i> , (2017), [133]
EGF-GNP	DU 145 cells	EGFR receptor	NTP irradiation showed selective apoptosis of cells that have undergone receptor mediated endocytosis.	Kim <i>et al.</i> , (2017), [137]
gGNRs	Radiotherapy to X-rays using actively targeted gGNRs; applied to mice bearing PC3-xenograft tumors and to PC3 cells	Not applicable	50% reduction in tumor volume after 2 months of treatment.	Khoo <i>et al.</i> , (2017), [139]
Chitosan-AuNP	A sandwich-type electrochemical immunosensor using anti-PSA was designed for detecting PSA.	Not applicable	The fabricated immunosensor demonstrated excellent sensitivity, stability, and a detection limit of 0.001ng/mL.	Suresh <i>et al.</i> , (2018), [129]
PANI/AuNP-PNT	Anti-PSA Ab immobilized on the modified PANI/AuNP-PNT pencil graphite electrode with HRP-anti PSA secondary antibody to form the sandwich immunoassay	Not applicable	Limit of detection was found out to be 0.68 ng/mL	Vural <i>et al.</i> , (2018), [130]
PSi-GNP	PSA was immobilized at different concentrations on	Not applicable	Enhanced PSA sensitivity with a limit of detection at 1 ng/mL	Rodriguez <i>et al.</i> , (2018), [126]

	the surface of the sandwich bioassay (NiCr electrode).			
GQDs-AuNRs	Standard PSA solutions were used. NPs immobilized on electrodes tested for efficiency (Anti-PSA.GQDs-AuNRs Vs. aptamer-GQDs-AuNRs).	Not applicable	Both had same limit of detection (LOD) of 0.14 ng/mL. The aptasensor advantages over the immunosensor were the stability, simplicity, cost effectiveness.	Srivastava <i>et al.</i> , (2018), [134]

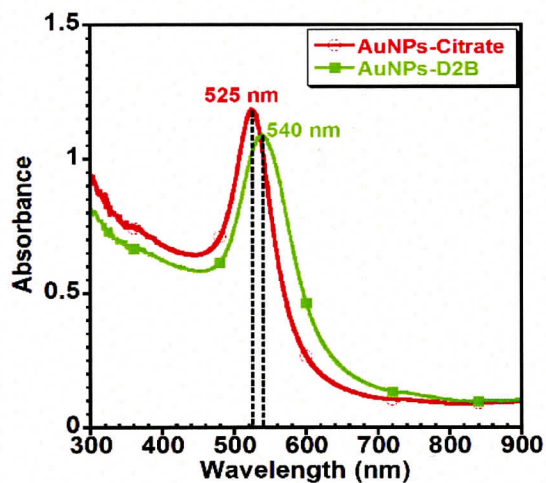


Figure 1: UV-Visible spectra of AuNPs-Citrate (~25 nm) before and after bioconjugation with D2B. Addition of D2B to AuNPs-citrate colloidal solution caused a green shift (higher wavelength) by about 15 nm in the UV-Vis spectra. This shift in wavelength might be due to the change in the refractive index around the AuNPs as a result to the attachment of D2B.

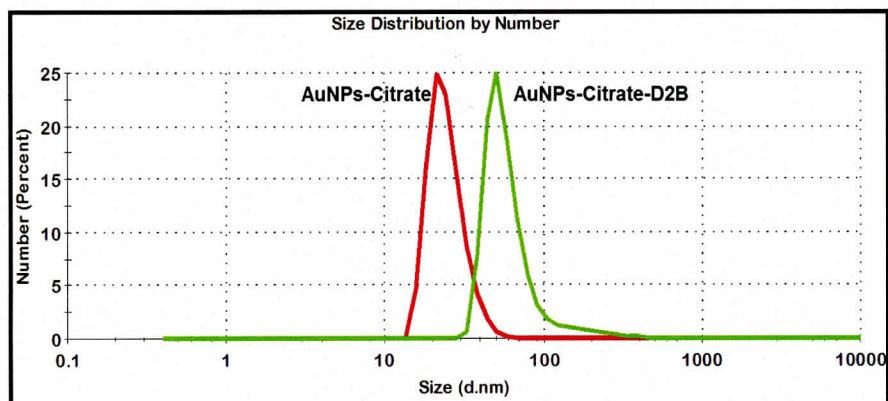


Figure 2: Size distribution by number from DLS on (~25 nm) AuNPs-Citrate before and after bioconjugation with D2B. An increase in the AuNPs size from ~25 to about ~ 63 nm confirms the successful conjugation of AuNPs-Citrate with D2B. The size variation is not quantitative and does not reflect the molar ration of D2B to AuNPs.

WST-1 Cell Proliferation Assay

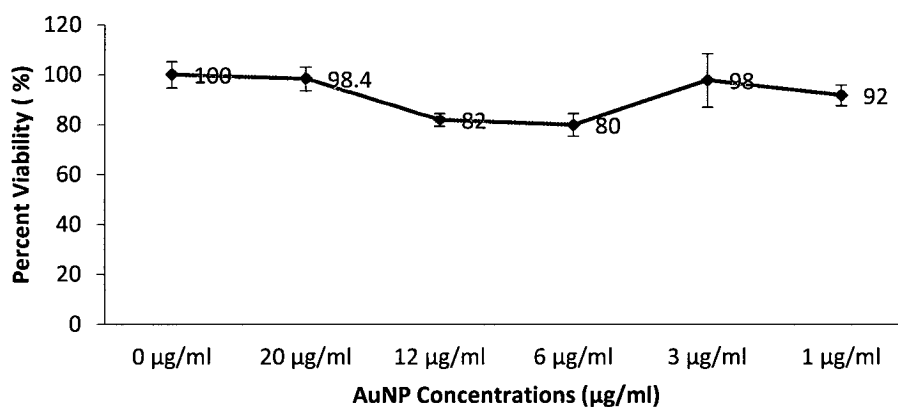


Figure 3: Effect of gold nanoparticles (AuNP) on PC3-PSMA proliferation. The graph shows the effect of different nanoparticle concentrations (µg/ml) on the cell proliferation of the prostate cancer cells, PC3-PSMA. The concentrations are as follows: control (dH₂O and RPMI), AuNP only (NP) =20 µg/mL, C₁=12 µg/mL, C₂= 6 µg/ml, C₃=3 µg/mL, C₄=1 µg/mL. Briefly, cells were seeded onto a 96-well plate and cultured for 24 hrs. Then they were treated with the variable gold nanoparticle concentrations for 4 hrs and the absorbance was read at 450nm.

WST-1 Cell Proliferation Assay

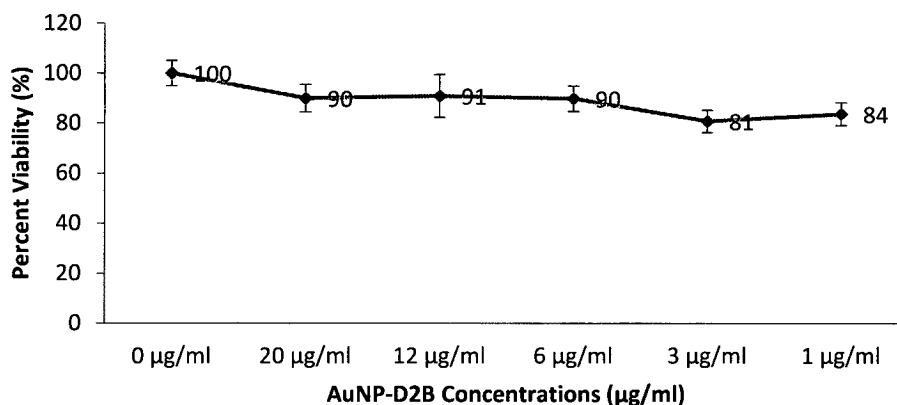


Figure 4: Effect of gold nanoparticles conjugated to D2B antibody (AuNP-D2B) on PC3-PSMA proliferation. The graph shows the effect of variable concentrations of AuNP-D2B, on the proliferation rate of the prostate cancer cells, PC3-PSMA. The concentrations are as follows: negative control (dH₂O only 20 µg/mL), positive control AuNP only =20 µg/mL, C₁=12 µg/mL, C₂= 6 µg/mL, C₃=3 µg/mL, C₄=1 µg/mL. Briefly, cells were seeded onto a 96-well plate and cultured for 24 hrs. Then they were treated with the variable gold nanoparticle concentrations for 4 hrs and the absorbance was read at 450 nm.

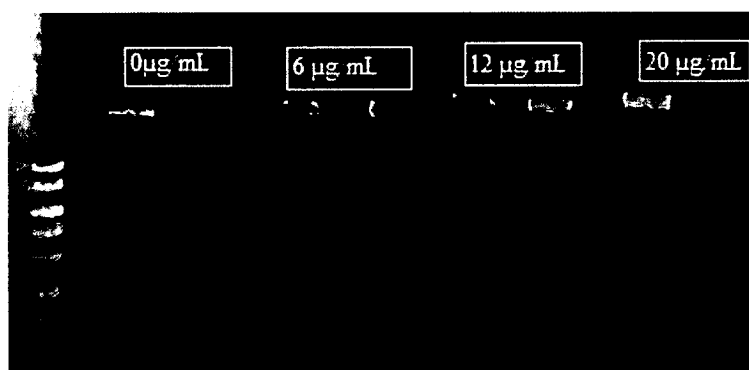


Figure 5: DNA analysis of the PC3-PSMA cells treated with increasing concentrations of AuNP-D2B. Each concentration (0, 6, 12, and 20 µg/mL) was done in duplicates. To evaluate whether the D2B conjugated gold nanoparticles (AuNP-D2B) induced apoptosis in the prostate cancer cells (PC3-PSMA), DNA fragmentation analysis was done using a 1% agarose gel electrophoresis and comparing the DNA profile of the treated cells to a 1kb molecular weight DNA ladder. The results show that increasing AuNP-D2B concentrations did not lead to DNA fragmentation and all wells were similar to the control.

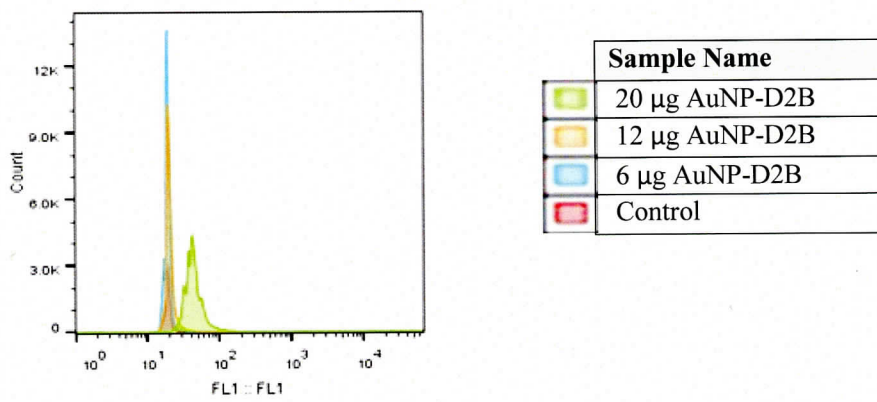


Figure 6: Typical representative histogram of AuNP-D2B binding to PC3-PSMA. PC3-PSMA cells (2×10^5) were incubated with increasing concentrations of Gold nanoparticles conjugated to D2B (0, 6, 12 and 20 $\mu\text{g/mL}$ of AuNP-D2B respectively) for 4 hrs. The samples were then read by flow cytometry using goat anti-mouse IgG secondary antibody- conjugated to FTIC (1:500). The control consisted of the PC3-PSMA cells with RPMI media only.

The histogram shows the fluorescence distribution of gated PC3-PSMA cells using logarithmic scale. Data represents a typical experiment ($n=3$). Fluorescence increased as AuNP-D2B concentration reached levels of 20 $\mu\text{g/mL}$. Plots were gated at 50,000 cells per sample.

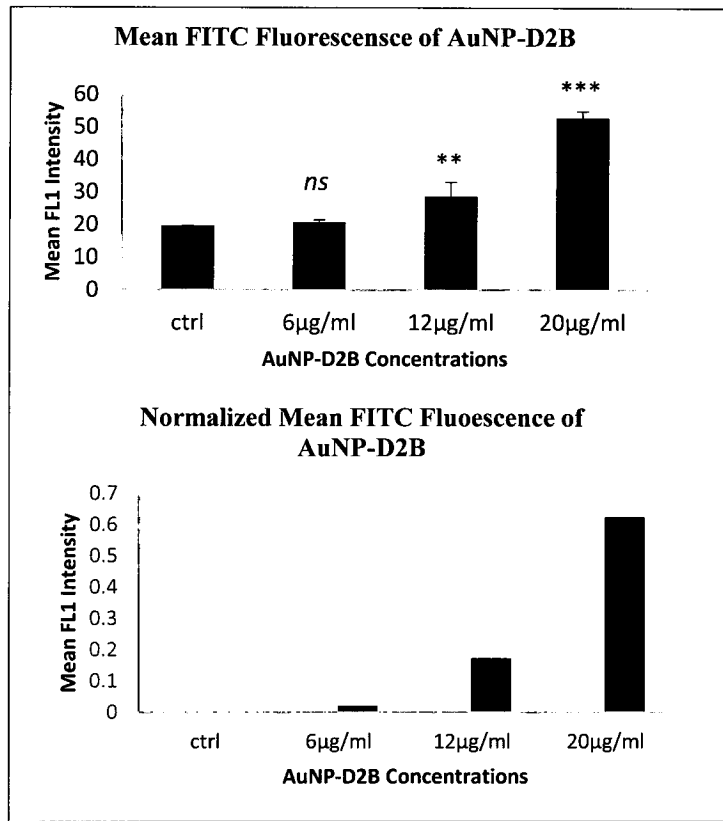


Figure 7: FACS analysis of AuNP-D2B binding to PC3-PSMA. PC3-PSMA cells (2×10^5) were incubated with increasing concentrations of gold nanoparticles conjugated to D2B (0, 6, 12 and 20 $\mu\text{g/ml}$ of AuNP-D2B respectively) for 4 hrs. Samples were then assessed by flow cytometry using FITC conjugated secondary antibody (1:500) against D2B which is eventually going to bind to PSMA receptors on the prostate cancer cells. The control consisted of the PC3-PSMA cells with RPMI media only. The bar graph shows the fluorescence intensity of the PC3-PSMA cells treated with AuNP-D2B. Data represents a typical experiment ($n=3$). Fluorescence increased as AuNP-D2B concentration increased (directly proportional). Plots were gated at 50,000 cells per sample. ($n=3$). (ns: non-significant difference)

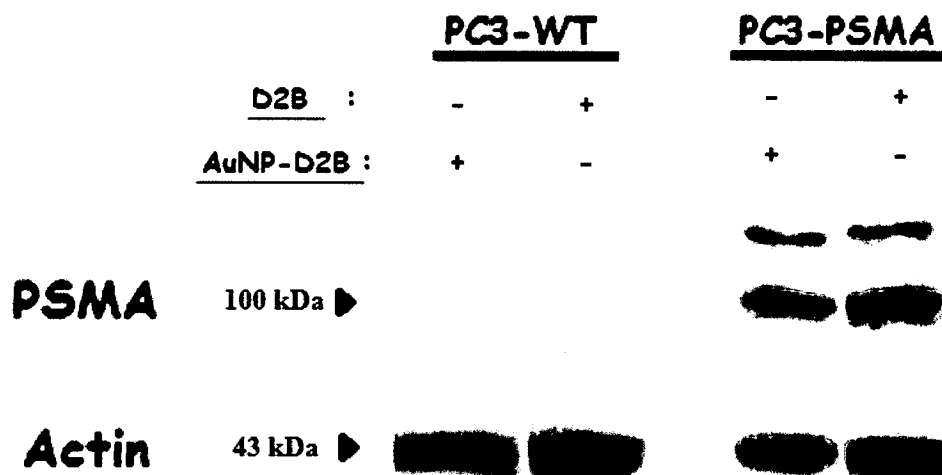


Figure 8: Western Blot Analysis for PSMA expression and AuNP-D2B binding. Western Blot image obtained after treating the cells, PC3-WT and PC3-PSMA (4×10^6 /lane), with bare D2B primary antibody or AuNP bound to D2B, for 4 hrs in serum free RPMI media. Both D2B concentrations and AuNP-D2B used, were $20 \mu\text{g/ml}$. Samples were incubated with 1:5000 secondary IgG conjugated to HRP. A molecular weight ladder was used to compare the resulting bands. Results obtained represent a typical experiment ($n=3$). No band was observed for the PC3-WT cells (PSMA⁻) and two very similar bands were observed for the PC3-PSMA cells treated with primary D2B alone or conjugated to AuNP.

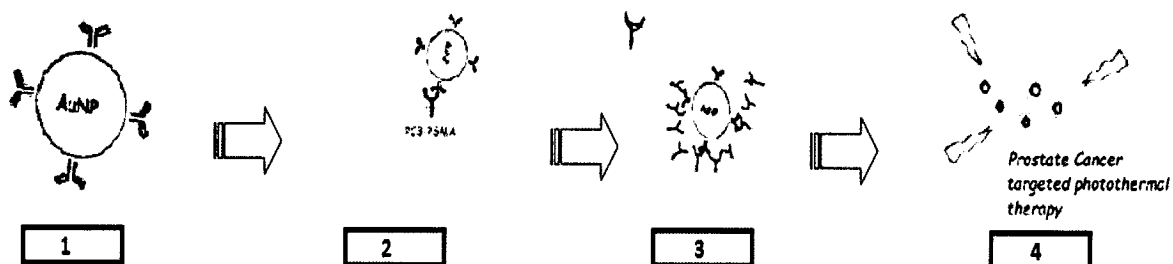


Figure 9: A stepwise schematic representation of a targeted photothermal therapy on PSMA expressing prostate cancer cells. Steps 1 and 2 represent an anti-PSMA antibody bound onto a gold nanoparticle that will bind to the prostate cancer cell (PC3-PSMA) surface when introduced intratumorally. Binding of the receptor to the antibody will initiate endocytosis of the complex, which will eventually lead to the accumulation of the AuNPs internally and this represented in step 3. Finally, in step 4, eradication of the prostate tumor would be through photothermal therapy (infrared radiation) that will excite the particles and cause a release of energy by heat generation and this hyperthermic environment will induce apoptosis of the prostate cancer cells.

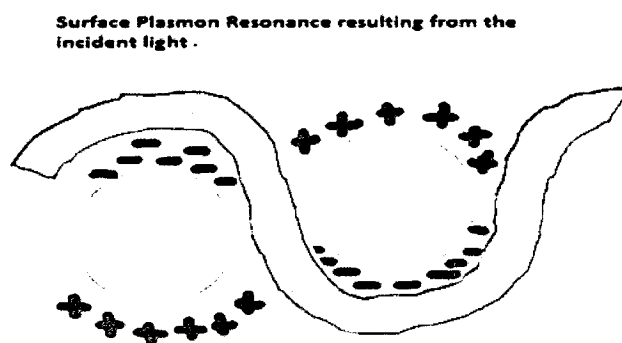


Figure 10: A schematic figure illustrating the surface plasmon resonance. When incident light encounters the nanoparticles, the electrons on the surface will undergo resonance causing their polarization. This resonance is translated into absorption of the light that results in an absorption band when characterizing the nanoparticles using UV-visible spectrophotometry.

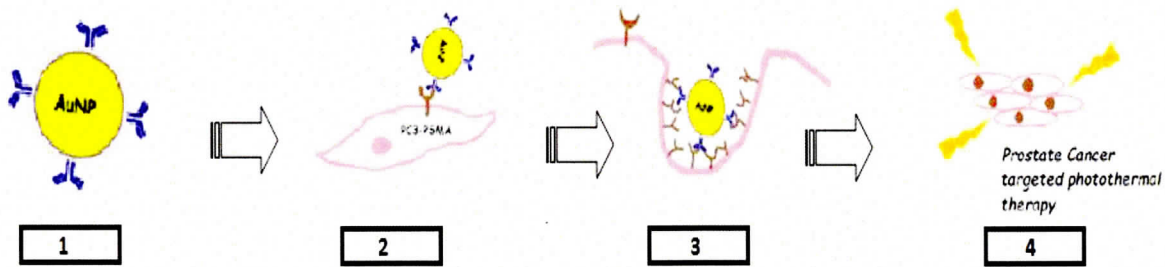


Figure 9: A stepwise schematic representation of a targeted photothermal therapy on PSMA expressing prostate cancer cells. Steps 1 and 2 represent an anti-PSMA antibody bound onto a gold nanoparticle that will bind to the prostate cancer cell (PC3-PSMA) surface when introduced intratumorally. Binding of the receptor to the antibody will initiate endocytosis of the complex, which will eventually lead to the accumulation of the AuNPs internally and this represented in step 3. Finally, in step 4, eradication of the prostate tumor would be through photothermal therapy (infrared radiation) that will excite the particles and cause a release of energy by heat generation and this hyperthermic environment will induce apoptosis of the prostate cancer cells.

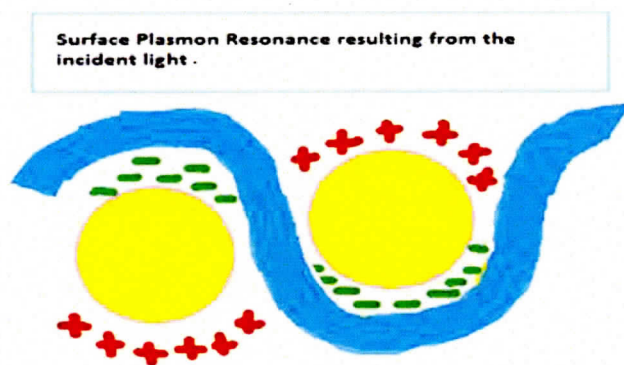


Figure 10: A schematic figure illustrating the surface plasmon resonance. When incident light encounters the nanoparticles, the electrons on the surface will undergo resonance causing their polarization. This resonance is translated into absorption of the light that results in an absorption band when characterizing the nanoparticles using UV-visible spectrophotometry.

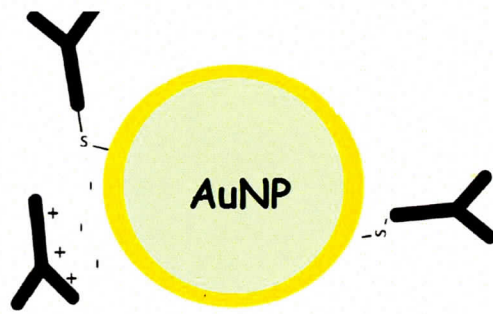


Figure 11: A representative image of the antibody binding onto the gold nanoparticles. Antibodies bind to nanoparticles by the thiol groups in the cysteine amino acid present in the antibody. Thiol attaches with a high affinity to the surface of the gold nanoparticles. Moreover, the amine groups at the (N-terminal) of the antibodies, binds ionically to the citrate molecules.

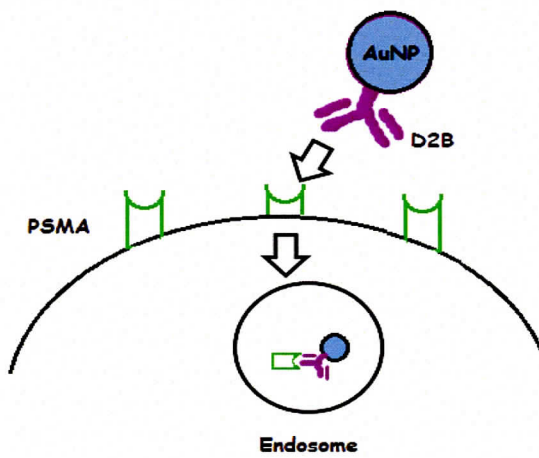


Figure 12: A schematic figure representation of the internalization of PSMA targeted AuNP-D2Bs. Ligand binding to PSMA receptors through either antibodies or peptides induces the activation of PSMA receptors and its consequent internalization through receptor mediated endocytosis.

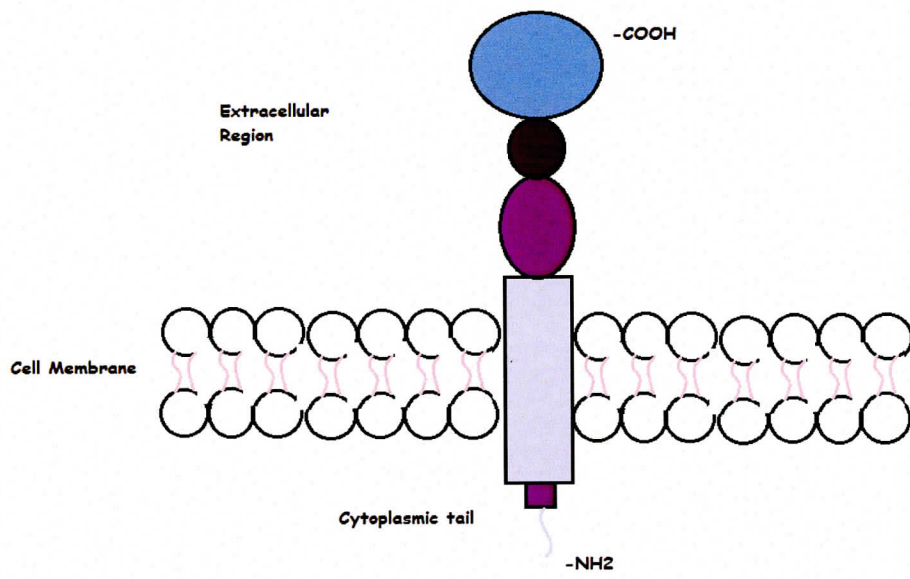


Figure 13: Figure sketch representing the PSMA Structure. PSMA is a type-II-transmembrane protein with a short NH₂-terminal cytoplasmic domain (CD), a hydrophobic transmembrane region (TM) and a large extracellular domain (ED).